Fig. 5

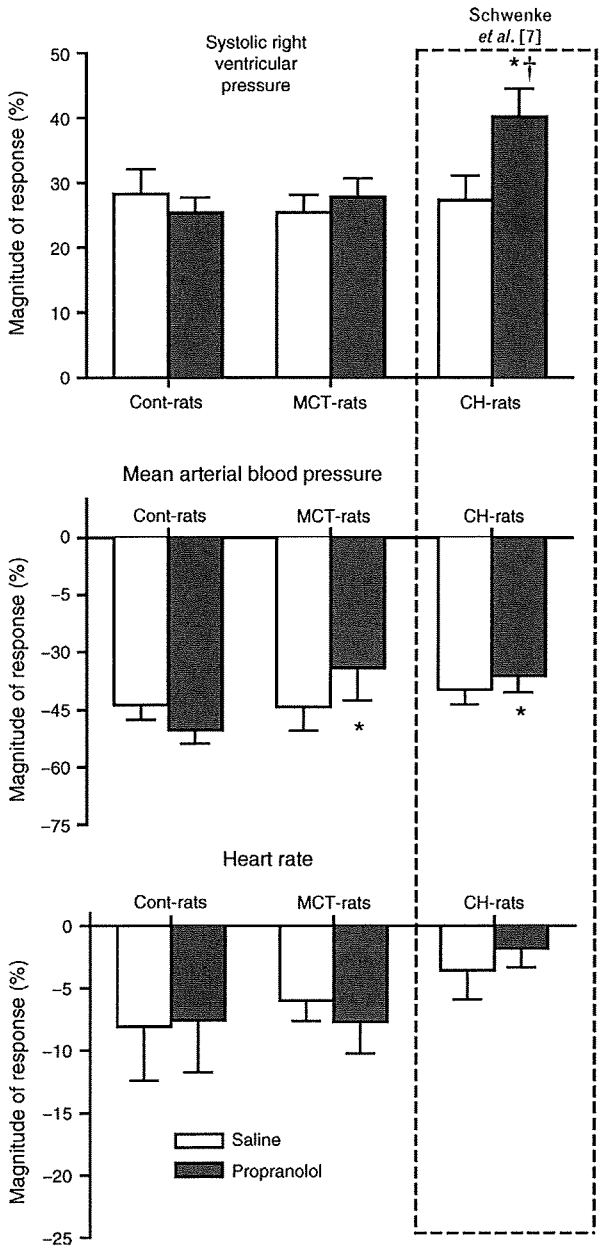

Hemodynamic responses (% change) of control rats (cont-rats; $n=7$), monocrotaline-treated rats (MCT-rats, $n=7$) and chronic hypoxic rats (chronic hypoxic rats; $n=5$) to acute hypoxia (8% O_2 for 4 min), before and after the i.v. administration of propranolol (2 mg/kg). *Significant difference in the magnitude of response between cont-rats and pulmonary hypertensive rats ($P<0.05$). †Significant response to propranolol ($P<0.01$). MCT, monocrotaline.

localized to the vessels that regulate pulmonary vascular resistance and generally have an internal diameter between 50 μm and less than 300 μm [8,26,27].

Although synchrotron radiation can identify gross changes in pulmonary blood flow distribution (vessels with an internal diameter ≥ 80 μm), one significant limitation of synchrotron radiation that we have previously discussed [7,8] is the inability to assess the integrity of the vascular wall in PAH and, thus, identify the basis for the change in internal vessel dimension and pulmonary blood flow. Indeed, synchrotron radiation is only able to measure the internal diameter of perfused vessels (assuming the vessel contains sufficient contrast medium) and is therefore a straightforward, albeit powerful, method for assessing gross anatomical changes in the pulmonary circulation of the hypertensive lung.

A reduction in the number of visibly opaque vessels in the hypertensive lung has been attributed to vessel 'pruning' or 'rarefaction' – a physical reduction in the total number of pulmonary arterioles [26,28–30], medial hypertrophy – encroachment of vascular smooth muscle into the vessel lumen, thereby impeding blood flow [4,13,31] and sustained vasoconstriction – reversible narrowing of the vessel lumen [32].

Although the literature implicates a combination of these structural changes in the pulmonary vasculature, the relative contribution of each one to the chronic elevation in vascular resistance may differ between MCT and chronic hypoxia models [4,5,33]. Van Suylen *et al.* [4] reported comparable increases in PAP for chronic hypoxic and MCT-rat models. Although medial thickening was well correlated, and could solely account for the increase in PAP in the MCT model, it alone could not account for the increase in PAP in the chronic hypoxia model. Van Suylen *et al.* [4] concluded that chronic hypoxia-induced PAH was likely attributable to both medial thickening and sustained vasoconstriction. More recently, Crossno *et al.* [5] showed that the therapeutic prevention of medial thickening (using rosiglitazone) associated with chronic hypoxia did not necessarily lead to a decrease in PAP because of the inability to repress sustained Rho kinase-mediated vasoconstriction.

Hypoxic pulmonary vasoconstriction in the rat

In this study, we used synchrotron radiation to assess the dynamic changes in vessel caliber in response to acute hypoxia (i.e. HPV). The results of this study concur with our previous reports [7,8] that showed, in cont-rats, all vessels with a diameter less than 500 μm, especially between 200 and 300 μm, constricted in response to acute hypoxia (8% O_2). Moreover, the acute HPV does not appear to be significantly altered following either MCT-induced or chronic hypoxia-induced PAH. The unique finding of this study, however, is that sympathetic modulation of the acute HPV is not modified by MCT, like it is with chronic hypoxia.

In spite of decades of research concerning the HPV, the exact mechanism(s) that govern acute HPV are yet to be fully elucidated, though various humoral (e.g. nitric

Copyright © Lippincott Williams & Wilkins. Unauthorized reproduction of this article is prohibited.

oxide) and neural pathways are likely to be involved (see Moudgil *et al.* [34] for a review). Hypoxia is a potent activator of pulmonary sympathetic nerve activity (SNA). The increase in SNA has been reported to attenuate the local vasoconstrictor effects of hypoxia via a β-adrenoceptor-mediated vasodilator mechanism, especially when the inspired level of O_2 is 8% O_2 or less [35,36].

We observed, previously [7,8] and in this study, that sympathetic β-adrenoceptor blockade (using propranolol) in cont-rats does not modify baseline vascular tone, but it does accentuate HPV of those vessels 200–300 μm in diameter. These results support the concept that modulation of the pulmonary vasculature by the sympathetic nervous system appears to be an important homeostatic response for limiting the magnitude of vasoconstriction under acute hypoxic conditions.

Perhaps one of the most fundamental differences between MCT and chronic hypoxia is that the action of MCT is effectively 'isolated' to the pulmonary endothelium, whereas chronic hypoxia has extensive adverse effects on the physiology of the whole organism, such as increasing sympathetic tone, increasing cardiac output, inducing polycythemia and locally causing systemic vasodilation and pulmonary vasoconstriction. In this study, we have demonstrated for the first time that chronic hypoxia, unlike MCT, enhances sympathetic modulation of the HPV. Specifically, we observed that β-receptor blockade in chronic hypoxic rats significantly accentuated the HPV, not only in the 200–300 μm vessels like that observed for cont-rats, but also in 100–200 μm vessels. These results indicate that sympathetic modulation of the HPV becomes critically important during chronic hypoxia.

Although the mechanism(s) responsible for alterations of the HPV in the hypertensive lung requires further research, we speculate that the altered regulation of HPV following chronic hypoxia may be attributable to an increase in sympathetic innervation of the pulmonary vasculature. Studies have shown that chronic hypoxia significantly increases β-receptor number within the lung [37,38] so that modulation of HPV by the sympathetic nervous system is enhanced following chronic hypoxia. Consequently, blockade of the β-adrenoceptor-mediated vasodilator mechanism in the chronic hypoxic lung will exacerbate the HPV [7]. In contrast, evidence in the literature suggests that MCT reduces pulmonary β-adrenergic receptor density [39] and sympathetic activity [40,41], though these effects have been associated with the development of right heart failure rather than the direct effect of MCT. Consequently, it is likely that in our study MCT may have reduced pulmonary β-receptor density and attenuated sympathetic tone so that the magnitude of HPV following propranolol administration was not accentuated, as observed in chronic hypoxic rats, but, if anything, perhaps slightly attenuated.

In summary, we have utilized the powerful resource of synchrotron radiation microangiography to show that the adverse changes in pulmonary blood flow distribution in the hypertensive lung are comparable between MCT and chronic hypoxia models. This is in contrast to the literature that shows that signaling pathways, and the subsequent vascular morphological changes, involved in the pathogenesis of PAH are likely to be different between the two models. We also demonstrated that the acute HPV was not altered in the hypertensive lung, though sympathetic modulation of pulmonary vasoreactivity becomes critically important in the chronic hypoxia model, but not the MCT-model. This is likely due to the impact that different pathomechanism pathways for each model have on the physiology of the whole organism. Both models of PAH represent specific types of PAH typically observed in humans and, therefore, such differences between the two PAH models should be considered in future studies, especially those studies investigating potential therapeutic interventions for a specific form of PAH.

Acknowledgements

This study was supported by the Department of Physiology, Otago University, New Zealand, and also in part by a Grant-in-Aid for Scientific Research (No. 16659210) and a Monash Synchrotron Fellowship (J.T.P.). We also acknowledge financial support from the access to Major Research Facilities Program, which is a component of the International Science Linkages Program (Australian Government). The synchrotron radiation experiments were performed at the BL28B2 in the SPring-8 with the approval of the Japan Synchrotron Radiation Research Institute (Proposal No. 2007A1538-NL2-NP).

There are no conflicts of interest.

References

1 Klinger JR, Hill NS. Right ventricular dysfunction in chronic obstructive pulmonary disease. Evaluation and management. *Chest* 1991; **99**:715–723.
2 Horstman DJ, Frank DU, Rich GF. Prolonged inhaled NO attenuates hypoxic, but not monocrotaline-induced, pulmonary vascular remodeling in rats. *Anesth Analg* 1998; **86**:74–81.
3 Raoul W, Wagner-Ballon O, Saber G, Hulin A, Marcos E, Giraudier S, *et al.* Effects of bone marrow-derived cells on monocrotaline- and hypoxia-induced pulmonary hypertension in mice. *Respir Res* 2007; **8**:8.
4 van Suylen RJ, Smits JF, Daemen MJ. Pulmonary artery remodeling differs in hypoxia- and monocrotaline-induced pulmonary hypertension. *Am J Resp Crit Care Med* 1998; **157**:1423–1428.
5 Crossno JT Jr, Garat CV, Reusch JE, Morris KG, Dempsey EC, McMurtry IF, *et al.* Rosiglitazone attenuates hypoxia-induced pulmonary arterial remodelling. *Am J Physiol (Lung Cell Mol Physiol)* 2007; **292**:L885–897.
6 Meyrick B, Gamble W, Reid L. Development of Crotalaria pulmonary hypertension: hemodynamic and structural study. *Am J Physiol* 1980; **239**:H692–H702.
7 Schwenke DO, Pearson JT, Kangawa K, Umetani K, Shirai M. Changes in macrovessel pulmonary blood flow distribution following chronic hypoxia: assessed using synchrotron radiation microangiography. *J Appl Physiol* 2008; **104**:88–96.
8 Schwenke DO, Pearson JT, Kangawa K, Umetani K, Shirai M. Imaging of the pulmonary circulation in the closed-chest rat using synchrotron radiation microangiography. *J Appl Physiol* 2007; **102**:787–793.

Copyright © Lippincott Williams & Wilkins. Unauthorized reproduction of this article is prohibited.

9 Archer S, Rich S. Primary pulmonary hypertension: a vascular biology and translational research 'Work in progress'. *Circulation* 2000; **102**:2781–2791.
10 Barbera JA, Peinado VI, Santos S. Pulmonary hypertension in COPD: old and new concepts. *Monaldi Arch Chest Dis* 2000; **55**:445–449.
11 Voelkel NF, Tuder RM. Hypoxia-induced pulmonary vascular remodeling: a model for what human disease? *J Clin Invest* 2000; **106**:733–738.
12 Laudi S, Steudel W, Jonscher K, Schoning W, Schniedewind B, Kaisers U, *et al.* Comparison of lung proteome profiles in two rodent models of pulmonary arterial hypertension. *Proteomics* 2007; **7**:2469–2478.
13 Schwenke DO, Tokudome T, Shirai M, Hosoda H, Horio T, Kishimoto I, Kangawa K. Exogenous ghrelin attenuates the progression of chronic hypoxia-induced pulmonary hypertension in conscious rats. *Endocrinology* 2008; **149**:237–244.
14 Yang X, Chen W, Li F. The change and distribution of endothelin-1 in lung of hypoxic pulmonary hypertension rat. *Hua Xi Yi Ke Da Xue Xue Bao* 2000; **31**:30–33.
15 Blumberg FC, Lorenz C, Wolf K, Sandner P, Riegger GA, Pfeifer M. Increased pulmonary prostacyclin synthesis in rats with chronic hypoxic pulmonary hypertension. *Cardiovasc Res* 2002; **55**:171–177.
16 Frasch HF, Marshall C, Marshall BE. Endothelin-1 is elevated in monocrotaline pulmonary hypertension. *Am J Physiol* 1999; **276**:L304–310.
17 Mathew R, Zeballos GA, Tun H, Gewitz MH. Role of nitric oxide and endothelin-1 in monocrotaline-induced pulmonary hypertension in rats. *Cardiovasc Res* 1995; **30**:739–746.
18 Mathew R, Gloster ES, Sundararajan T, Thompson CI, Zeballos GA, Gewitz MH. Role of inhibition of nitric oxide production in monocrotaline-induced pulmonary hypertension. *J Appl Physiol* 1997; **82**:1493–1498.
19 Xue C, Rengasamy A, Le Cras TD, Koberna PA, Dailey GC, Johns RA. Distribution of NOS in normoxic vs. hypoxic rat lung: upregulation of NOS by chronic hypoxia. *Am J Physiol (Lung Cell Mol Physiol)* 1994; **267**:L667–L678.
20 Shirai M, Pearson JT, Shimouchi A, Nagaya N, Tsuchimochi H, Ninomiya I, Mori H. Changes in functional and histological distributions of nitric oxide synthase caused by chronic hypoxia in rat small pulmonary arteries. *Br J Pharmacol* 2003; **139**:899–910.
21 Le Cras TD, Xue C, Rengasamy A, Johns RA. Chronic hypoxia upregulates endothelial and inducible NO synthase gene and protein expression in rat lung. *Am J Physiol (Lung Cell Mol Physiol)* 1996; **270**:L164–170.
22 Sato K, Rodman DM, McMurtry IF. Hypoxia inhibits increased ET_B receptor-mediated NO synthesis in hypertensive rat lungs. *Am J Physiol (Lung Cell Mol Physiol)* 1999; **276**:L571–L581.
23 Maruyama J, Maruyama K. Impaired nitric oxide-dependent responses and their recovery in hypertensive pulmonary arteries of rats. *Am J Physiol* 1994; **266**:H2476–H2488.
24 Crawley DE, Zhao L, Giembycz MA, Liu S, Barnes PJ, Winter RJ, Evans TW. Chronic hypoxia impairs soluble guanylyl cyclase-mediated pulmonary arterial relaxation in the rat. *Am J Physiol* 1992; **263**:L325–L332.
25 Murata T, Yamawaki H, Hori M, Sato K, Ozaki H, Karaki H. Hypoxia impairs endothelium-dependent relaxation in organ cultured pulmonary artery. *Eur J Pharmacol* 2001; **421**:45–53.
26 Hislop A, Reid L. New findings in pulmonary arteries of rats with hypoxia-induced pulmonary hypertension. *Br J Exp Pathol* 1976; **57**:542–554.
27 Yamashita T, Kawashima S, Ozaki M, Namiki M, Shinohara M, Inoue N, *et al.* In vivo angiographic detection of vascular lesions in apolipoprotein E-knockout mice using a synchrotron radiation microangiography system. *Circ J* 2002; **66**:1057–1059.
28 Fried R, Reid LM. Early recovery from hypoxic pulmonary hypertension: a structural and functional study. *J Appl Physiol* 1984; **57**:1247–1253.
29 Hislop A, Reid L. Normal structure and dimensions of the pulmonary arteries in the rat. *J Anat* 1978; **125**:71–83.
30 Meyrick B, Reid L. The effect of continued hypoxia on rat pulmonary arterial circulation. An ultrastructural study. *Lab Invest* 1978; **38**:188–200.
31 Sasaki S, Kobayashi N, Dambara T, Kira S, Sakai T. Structural organization of pulmonary arteries in the rat lung. *Anat Embryol (Berl)* 1995; **191**:477–489.
32 Nagaoka T, Fagan KA, Gebb SA, Morris KG, Suzuki T, Shimokawa H, *et al.* Inhaled Rho kinase inhibitors are potent and selective vasodilators in rat pulmonary hypertension. *Am J Resp Crit Care Med* 2005; **171**:494–499.
33 Rabinovitch M, Gamble W, Nadas AS, Miettinen OS, Reid L. Rat pulmonary circulation after chronic hypoxia: hemodynamic and structural features. *Am J Physiol* 1979; **236**:H818–827.
34 Moudgil R, Michelakis ED, Archer SL. Hypoxic pulmonary vasoconstriction. *J Appl Physiol* 2005; **98**:390–403.
35 Shirai M, Matsukawa K, Nishiura N, Kawaguchi AT, Ninomiya I. Changes in efferent pulmonary sympathetic nerve activity during systemic hypoxia in anesthetized cats. *Am J Physiol (Regul Integr Comp Physiol)* 1995; **269**:R1404–1409.
36 Shirai M, Shindo T, Ninomiya I. Beta-adrenergic mechanisms attenuated hypoxic pulmonary vasoconstriction during systemic hypoxia in cats. *Am J Physiol (Heart Circ Physiol)* 1994; **266**:H1777–1785.
37 Birnkrant DJ, Davis PB, Ernsberger P. Visualization of high- and low-affinity beta-adrenergic receptors in rat lung: upregulation by chronic hypoxia. *Am J Physiol* 1993; **265**:L389–394.
38 Winter RJ, Dickinson KE, Rudd RM, Sever PS. Tissue specific modulation of beta-adrenoceptor number in rats with chronic hypoxia with an attenuated response to down-regulation by salbutamol. *Clin Sci (Lond)* 1986; **70**:159–165.
39 Brown L, Miller J, Dagger A, Sernia C. Cardiac and vascular responses after monocrotaline-induced hypertrophy in rats. *J Cardiol Pharmacol* 1998; **31**:108–115.
40 Tucker A, Bryant SE, Frost HH, Migally N. Chemical sympathectomy and serotonin inhibition reduce monocrotaline-induced right ventricular hypertrophy in rats. *Can J Physiol Pharmacol* 1983; **61**:356–362.
41 Yamada Y, Okumura K, Hashimoto H, Ito T, Satake T. Altered myocardial acetylcholine and norepinephrine concentrations in right ventricular hypertrophy and failure. *Heart Vessels* 1991; **6**:150–157.

Copyright © Lippincott Williams & Wilkins. Unauthorized reproduction of this article is prohibited.

© The American Society of Gene Therapy

Intratracheal Gene Transfer of Adrenomedullin Using Polyplex Nanomicelles Attenuates Monocrotaline-induced Pulmonary Hypertension in Rats

Mariko Harada-Shiba[1], Itaru Takamisawa[1], Kanjiro Miyata[2,3], Takehiko Ishii[2,3], Nobuhiro Nishiyama[3,4], Keiji Itaka[3,4], Kenji Kangawa[5], Fumiki Yoshihara[6], Yujiro Asada[7], Kinta Hatakeyama[7], Noriya Nagaya[8] and Kazunori Kataoka[3,4,9]

[1]Department of Bioscience, National Cardiovascular Center Research Institute, Suita, Japan; [2]Department of Bioengineering, Graduate School of Engineering, The University of Tokyo, Tokyo, Japan; [3]Center for NanoBio Integration, The University of Tokyo, Tokyo, Japan; [4]Division of Clinical Biotechnology; Center for Disease Biology and Integrative Medicine, Graduate School of Medicine, The University of Tokyo, Tokyo, Japan; [5]National Cardiovascular Center Research Institute, Suita, Japan; [6]Division of Hypertension and Nephrology, National Cardiovascular Center, Suita, Japan; [7]Department of Pathology, Faculty of Medicine, University of Miyazaki, Miyazaki, Japan; [8]Department of Regenerative Medicine, National Cardiovascular Center Research Institute, Suita, Japan; [9]Department of Materials Engineering, Graduate School of Engineering, The University of Tokyo, Tokyo, Japan

Pulmonary arterial hypertension (PAH) is a life-threatening disease characterized by progressive PAH and right ventricular failure. Despite recent advances in therapeutic approaches using prostanoids, endothelin antagonists, and so on, PAH remains a challenging condition. To develop a novel therapeutic approach, we have established a nonviral gene delivery system of poly(ethylene glycol) (PEG)-based block catiomers, which form a polyplex nanomicelle with a nanoscaled core–shell structure in the presence of DNA. The polyplex nanomicelle from PEG-*b*-poly{*N*-[*N*-(2-aminoethyl)-2-aminoethyl]aspartamide} (PEG-*b*-P[Asp(DET)]), having ethylenediamine units at the side chain, showed ~100-fold increase in luciferase transgene expression activity in mouse lung via intratracheal administration with a minimal toxicity compared with the polyplex from linear poly(ethylenimine) (LPEI). The transfection activity was highest on day 3 after administration and remained detectable until day 14. PEG-*b*-P[Asp(DET)] polyplex nanomicelles were formulated with a therapeutic plasmid bearing the human adrenomedullin (*AM*) gene and intratracheally administered to rats with monocrotaline-induced pulmonary hypertension. The right ventricular pressure significantly decreased 3 days after administration as confirmed by a notable increase of pulmonary human AM mRNA levels. Intratracheal administration of PEG-*b*-P[Asp-(DET)] polyplex nanomicelles showed remarkable therapeutic efficacy with PAH animal models without compromising biocompatibility.

Received 29 July 2008; accepted 9 March 2009; published online 31 March 2009. doi:10.1038/mt.2009.63

INTRODUCTION

Idiopathic pulmonary arterial hypertension (PAH) is a rare disease characterized by a progressive increase in pulmonary vascular resistance, leading to right heart failure and death.[1] Recent advances in therapeutic approaches to PAH show promising targeting pathways believed to play critical pathogenic or pathophysiologic roles;[2] however, despite these findings, PAH remains a challenging condition.[3]

Adrenomedullin (AM), a peptide isolated from human pheochromocytoma,[4] has multiple beneficial effects on cardiovascular tissues, including a powerful hypotensive effect.[5] Moreover, AM is indicated for PAH because of its prodilatory effects and the abundance of AM receptors in the lung.[6] Inhalation of AM was reported to ameliorate PAH in animal models[7] as well as in PAH patients without inducing systemic hypotension, but this effect was transient.[8] To overcome these barriers, a new, efficacious, and long-lasting AM therapy for PAH is warranted.

Gene therapy is one of the strategic approaches to continuously supply therapeutic peptides or proteins to target tissues.[6] Gene delivery to the lung via inhalation can avoid many problems associated with intravenous delivery, such as immediate nuclease degradation in the blood stream and the difficulty associated with penetrating endothelial barriers. In this regard, AM-based gene therapy through intratracheal route for PAH may have a promise.[7] Successful gene delivery via inhalation strongly depends on the development of advanced gene vectors to protect the therapeutic plasmid, provide site-specific targeting, and effectively release these plasmids for the desired pharmacological effect.

To develop a novel gene therapy system, we utilized our established polymeric library consisting of poly(ethylene glycol) (PEG)-based block catiomers, which form core–shell polyplex nanomicelles with core sequestration of the therapeutic plasmid.[9,10]

Correspondence: Mariko Harada-Shiba, Department of Bioscience, National Cardiovascular Center Research Institute, 5-7-1 Fujishirodai, Suita, Osaka 565-8565, Japan. E-mail: mshiba@ri.ncvc.go.jp

© The American Society of Gene Therapy

These polyplex nanomicelles are well dispersed even in aqueous media containing serum proteins and protect plasmid DNA from degradation by nuclease *in vivo*.[11–13] We recently developed P[Asp(DET)], a poly(aspartamide) derivative bearing an *N*-(2-aminoethyl)aminoethyl group as the side chain, that showed improved transfection efficiency and biocompatibility compared to linear poly(ethylenimine) (LPEI).[14] The PEG-based block cationomer with P[Asp(DET)] was applied *in vivo* to deliver therapeutic plasmids for a murine, skull bone defect model and a rabbit carotid artery with neointima model; its successful therapeutic efficacy with these mammalian studies provided the impetus for expanded application into the treatment of intractable diseases suited for gene therapy.[15,16]

In this paper, we report advanced, pulmonary transfection efficiencies using intratracheally inhaled PEG-*b*-P[Asp(DET)] polymeric nanomicelles without compromising biocompatibility. The intratracheal administration of the *AM* gene by PEG-*b*-P[Asp-(DET)] polyplex nanomicelles reduced right ventricular pressure in PAH animal models without inducing inflammation, suggesting its suitability as a vector for translational research.

RESULTS

Reporter gene transfer using PEG-*b*-P[Asp(DET)] via intratracheal administration

Plasmids bearing the luciferase reporter gene were formulated with PEG-*b*-P[Asp(DET)] (N/P = 80) and LPEI (N/P = 6) and were sprayed intratracheally into ICR mice. Here, N/P ratio refers to the unit molar ratio of the amino group in the polymer to the phosphate group in the plasmid DNA. After 1 day, the mice were killed and the pulmonary tissues were harvested to quantify luciferase activity. PEG-*b*-P[Asp(DET)] polyplex nanomicelles showed nearly a 100-fold increase in luciferase levels than the LPEI controls (**Figure 1**). **Figure 2** shows the time-dependent changes of luciferase gene expression in the pulmonary tissue with PEG-*b*-P[Asp(DET)] polyplex nanomicelles. Luciferase activity was highest on day 3, and remained detectable until day 14. To elucidate the effect of PEG-*b*-P([Asp(DET)]/pLuc N/P ratios on luciferase gene expression, a series of the nanomicelles formulated under the varying N/P ratios (20, 40, and 80) were also examined. **Figure 3** shows an ~50-fold increase in luciferase expression from N/P = 20 to N/P = 80 over a 3-day period. Next, PEG-*b*-P[Asp(DET)] polyplex nanomicelles loaded with plasmid DNA bearing the yellow fluorescence protein (YFP) gene (N/P = 80) or LPEI/pYFP polyplexes (N/P = 6) were sprayed intratracheally in ICR mice. After 1 day, the pulmonary tissue was harvested and the YFP gene expression was visualized by fluorescence microscopy (**Figure 4**). Significantly higher fluorescence intensity was clearly seen in the lungs treated with the PEG-*b*-P[Asp(DET)] polyplex nanomicelle than the LPEI polyplexes; moreover, YFP fluorescence activity was distinctly visible for the animals treated with PEG-*b*-P[Asp(DET)] polyplex micelles in the secondary bronchi and lower pulmonary generations. To evaluate the toxicity, immunohistochemistry was conducted on the lung tissues after the transfection of LPEI/pLuc controls (N/P = 6) (**Figure 5a–c**) or PEG-*b*-P[Asp(DET)]/pLuc (N/P = 80) (**Figure 5d–f**). The lung administered with LPEI/pLuc showed moderate infiltration of neutrophils at the

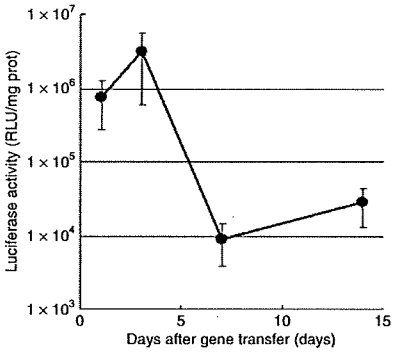

Figure 2 Time-dependent changes in gene expression after intratracheal administration of PEG-*b*-P[Asp(DET)] polyplex nanomicelle loaded with luciferase gene. The mice (five mice per group) were anesthetized and the polyplex nanomicelle was administered intratracheally. After the indicated time, the lung tissues were harvested, homogenized, and measured for luciferase activity (mean ± SEM, *N* = 5). PEG-*b*-P[Asp(DET)], PEG-*b*-poly{*N*-[*N*-(2-aminoethyl)-2-aminoethyl]aspartamide}.

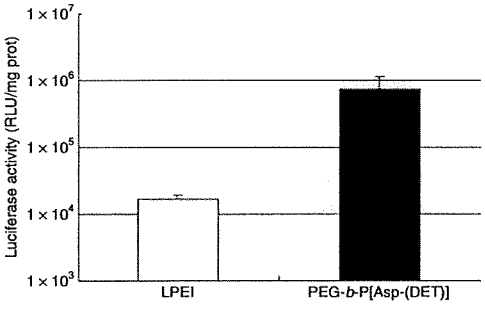

Figure 1 Luciferase gene expression by intratracheal administration of LPEI polyplex (N/P = 6) or PEG-*b*-P[Asp(DET)] polyplex nanomicelle (N/P = 80). Samples of the polyplex and the polyplex nanomicelle were prepared before the administration and left for 1 day. The mice (five mice per group) were anesthetized and the polyplex or the polyplex nanomicelle was administered intratracheally. At 24 hour postadministration, the lung tissues were harvested, homogenized, and measured for luciferase activity (mean ± SEM, *N* = 5). LPEI, linear poly(ethylenimine); PEG-*b*-P[Asp(DET)], PEG-*b*-poly{*N*-[*N*-(2-aminoethyl)-2-aminoethyl]aspartamide}.

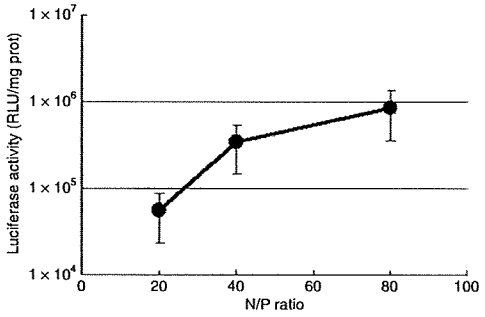

Figure 3 Charge-ratio-dependent changes in gene expression after intratracheal administration of the PEG-*b*-P[Asp(DET)] polyplex nanomicelle loaded with luciferase gene. The mice (five mice per group) were anesthetized and the polyplex nanomicelle was administered intratracheally. At 3 days postadministration, the lung tissues were harvested, homogenized, and measured for luciferase activity (mean ± SEM, *N* = 5). PEG-*b*-P[Asp(DET)], PEG-*b*-poly{*N*-[*N*-(2-aminoethyl)-2-aminoethyl]aspartamide}.

© The American Society of Gene Therapy

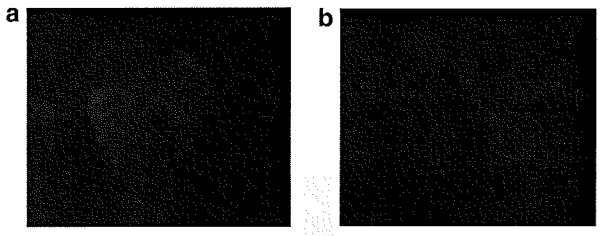

Figure 4 Fluorescence photographs of lungs transfected by intratracheal administration of YFP gene using PEG-*b*-P[Asp(DET)] polyplex nanomicelle or LPEI polyplex. (**a**) PEG-*b*-P[Asp(DET)] polyplex nanomicelle (N/P = 80), (**b**) LPEI polyplex (N/P = 6). The lung specimens were observed under a fluorescence microscope (SZX12; Olympus). LPEI, linear poly(ethylenimine); PEG-*b*-P[Asp(DET)], PEG-*b*-poly{*N*-[*N*-(2-aminoethyl)-2-aminoethyl]aspartamide}.

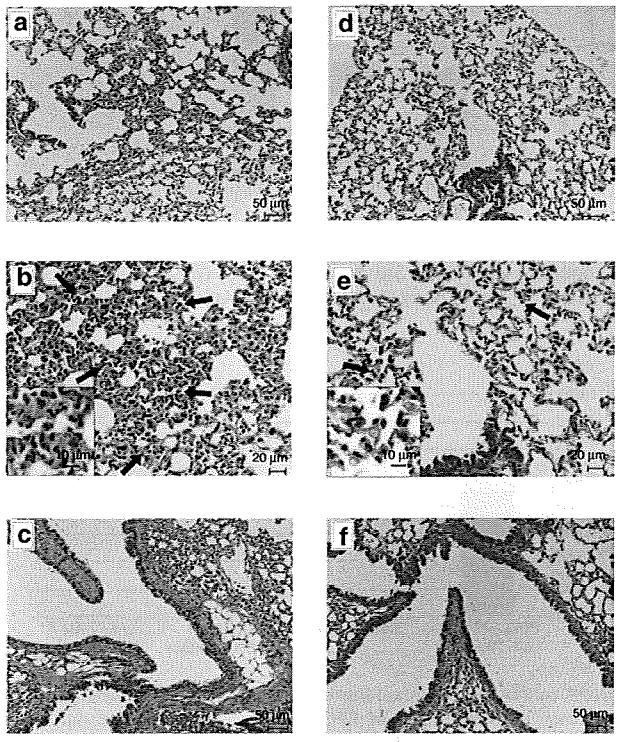

Figure 5 Representative photomicrographs of lung tissues 7 days postintratracheal administration of LPEI/pLuc (N/P = 6) (**a–c**) or PEG-*b*-P[Asp(DET)]/pLuc (N/P = 80) (**d–f**). The terminal bronchiole and alveoli of the lungs administered with LPEI polyplex (**a,b**) and PEG-*b*-P[Asp(DET)] polyplex nanomicelle (**d,e**) are shown. The neutrophil infiltration is indicated with arrows in the photomicrographs with higher magnification (**b,e**). Each inset is the picture with higher magnification. The bronchus of the lungs administered with LPEI polyplex (**c**) and PEG-*b*-P[Asp(DET)] polyplex nanomicelle (**f**) are also shown. LPEI, linear poly(ethylenimine); PEG-*b*-P[Asp(DET)], PEG-*b*-poly{*N*-[*N*-(2-aminoethyl)-2-aminoethyl]aspartamide}.

terminal bronchiole and alveoli as indicated (**Figure 5a,b**). However, the lung administered with PEG-*b*-P[Asp(DET)]/pLuc, neutrophilic infiltration was scattered and minimal or absent (**Figure 5d,e**). No apparent inflammatory infiltrate was observed in the bronchus of the both groups (**Figure 5c,f**). The findings thereby supported increased biocompatibility with the PEG-*b*-P[Asp(DET)] polyplex micelle. To further evaluate the toxicity of the gene carrier systems, mRNA levels of inflammatory cytokines in the pulmonary tissue were measured using real-time reverse transcriptase (RT)-PCR. A nontreated cohort was used as a control. Proinflammatory cytokine mRNA levels did not increase for intratracheally administered naked pLuc in saline or the PEG-*b*-P[Asp(DET)] polyplex micelles; however, LPEI/pLuc polyplexes revealed a twofold increase in TNF-α, interleukin (IL)-6, IL-10, and Cox-2 compared to the control (**Figure 6a–d**). Notably, PEG-*b*-P[Asp(DET)]/pLuc proinflammatory levels were statistically similar to the negative control cohorts in TNF-α, IL-6, IL-10, and Cox-2 mRNA levels.

Effect of *AM* gene transfer by PEG-*b*-P[Asp(DET)] polyplex nanomicelle in a rat model of PAH

After 4 weeks of monocrotaline injection, right ventricular pressure was increased to twice of the normal value (**Figure 7**). Notably, right ventricular pressure was decreased significantly by an intratracheal spray of the PEG-*b*-P[Asp(DET)] polyplex nanomicelle loaded with the expression vector of AM (N/P = 40). On the other hand, right ventricular pressure did not change significantly after administration of naked plasmid encoding the *AM* gene in saline or the LPEI polyplex loaded with the *AM* gene, or the polyplex nanomicelle loaded with the luciferase gene. The mRNA levels of human AM in the lung were measured by real-time RT-PCR (**Figure 8**). The lung transfected with the polyplex nanomicelle loaded with the expression vector of AM had high levels of AM mRNA. Alternatively, the levels were much lower in the lung transfected with the LPEI polyplex loaded with the expression vector of AM. The lung transfected with the polyplex nanomicelle loaded with the luciferase gene or with the naked *AM* gene in saline showed no expression of human AM.

DISCUSSION

The large number of human diseases presenting poor prognoses and limited efficacy with current therapeutic regimens necessitates the advent of alternative approaches. PAH is such a disease without a highly efficacious therapeutic regimen.[17] PAH patients are currently treated with a variety of drugs including prostacyclin, prostacyclin analogues, calcium channel blockers, nitric-oxide inhalation, angiotensin-converting enzyme inhibitors, endothelin receptor antagonists, and phosphodiesterase type 5 inhibitors; in severe cases lung transplantation and subsequent immunosuppression are necessary.[17] However, promising alternative therapies for PAH have been recently reported. For example, Champion *et al.* reported that adenoviral gene transfer of endothelial nitric-oxide synthase to the lungs of endothelial nitric-oxide synthase knockout mice ameliorates the symptoms of PAH.[18] Champion *et al.* also reported that adenoviral gene transfer of calcium gene-related peptide attenuates the symptoms of PAH.[19] Nagaya *et al.* reported that transfection of human prostacyclin synthase using hemagglutinating virus of Japan–liposomes ameliorates monocrotaline-induced PAH.[20] However, in these attempts, viral or viral-related vectors were used for the delivery of therapeutic genes and these gene carriers have the potential for immunogenicity and inflammatory response. In diseases where a single dose can cure or provide palliative care, viral vectors may be suitable; however, PAH therapy requires repeated

© The American Society of Gene Therapy

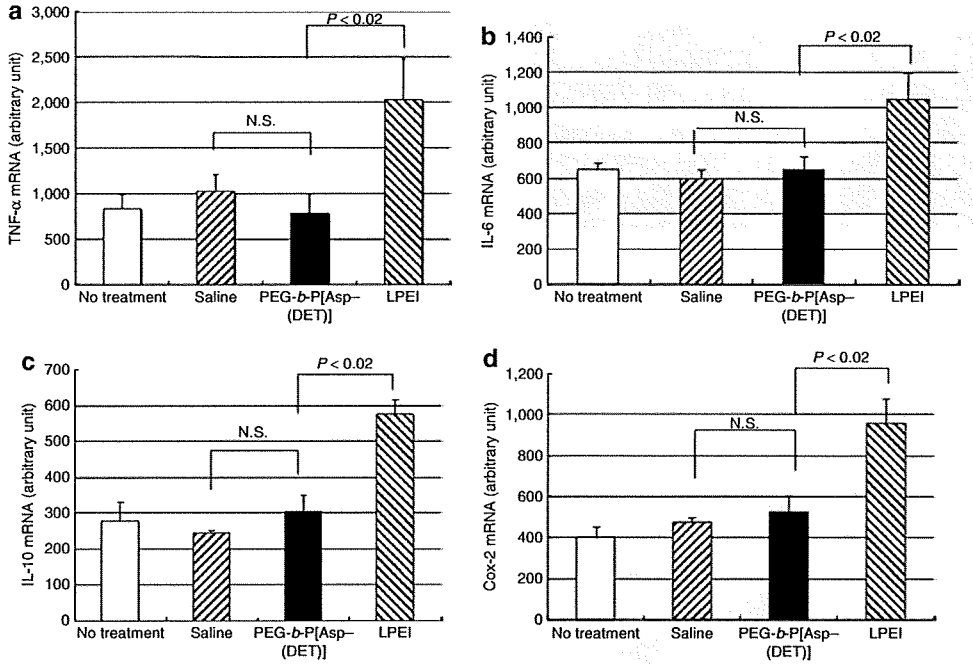

Figure 6 mRNA expression of inflammatory cytokines in lung tissues 7 days postintratracheal administration of luciferase gene in saline; LPEI polyplex with luciferase gene (N/P = 6); or PEG-*b*-P[Asp(DET)] polyplex nanomicelle with luciferase gene (N/P = 80) (mean ± SEM, $N = 4$). (**a**) TNF-α, (**b**) IL-6, (**c**) IL-10, (**d**) Cox-2. IL, interleukin; LPEI, linear poly(ethylenimine); TNF, tumor necrosis factor; PEG-*b*-P[Asp(DET)], PEG-*b*-poly{*N*-[*N*-(2-aminoethyl)-2-aminoethyl]aspartamide}.

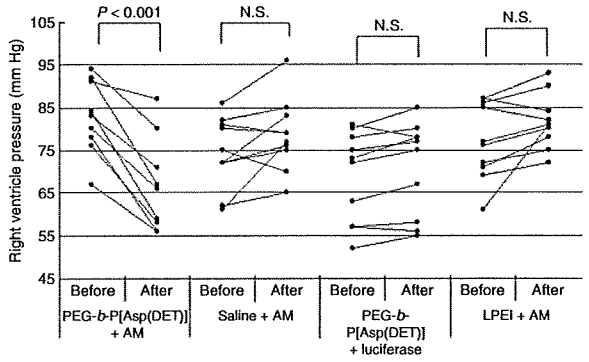

Figure 7 Effect of gene transfer on the right ventricle pressure in the PAH rat model. At 4 weeks after subcutaneous monocrotaline injection, a hemodynamic study was performed to measure the RV pressure indicated as "Before". The PEG-*b*-P[Asp(DET)] polyplex nanomicelle loaded with AM expression vector; AM expression vector in saline; PEG-*b*-P[Asp(DET)] polyplex micelle loaded with luciferase gene; or the LPEI polyplex loaded with AM expression vector were sprayed intratracheally. Three days later, a hemodynamic study was performed again to measure the RV pressure indicated as "After". AM, adrenomedullin; LPEI, linear poly(ethylenimine); PAH, pulmonary arterial hypertension; PEG-*b*-P[Asp(DET)], PEG-*b*-poly{*N*-[*N*-(2-aminoethyl)-2-aminoethyl]aspartamide}; RV, right ventricular.

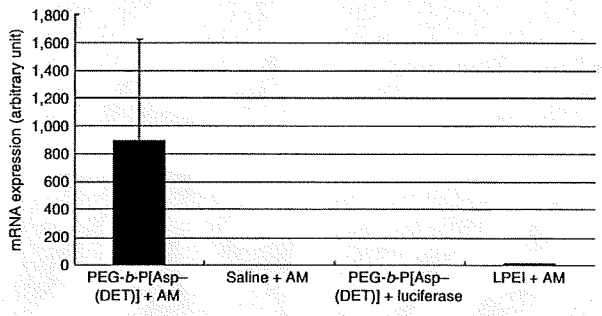

Figure 8 mRNA expression of human AM in the PAH rat model postintratracheal administration of PEG-*b*-P[Asp(DET)] polyplex nanomicelles loaded with the AM expression vector; AM expression vector in saline; PEG-*b*-P[Asp(DET)] polyplex nanomicelles loaded with the luciferase gene; or LPEI polyplexes loaded with the AM expression vector. Rats were transfected intratracheally at 4 weeks after subcutaneous monocrotaline injection. Three days later, lungs were harvested, homogenized, and measured for AM mRNA using real-time RT-PCR (mean ± SEM, $N = 4$). AM, adrenomedullin; LPEI, linear poly(ethylenimine); PAH, pulmonary arterial hypertension; PEG-*b*-P[Asp(DET)], PEG-*b*-poly{*N*-[*N*-(2-aminoethyl)-2-aminoethyl]aspartamide}.

administrations for efficacy, hence the utility of viral or viral-based gene therapy is contraindicated.

Alternatively, nonviral gene carriers have been recognized with several advantages over viral vectors in terms of safety, immunogenicity, and ease of manufacture. To develop a method of gene therapy suitable for clinical translation, four primary factors must be clearly addressed: (i) the gene carrier, (ii) the therapeutic gene, (iii) the route of administration, and (iv) patient compliance. In this study, we chose to further explore the promising (i) PEG-*b*-P[Asp(DET)] polyplex nanomicelle nonviral gene carrier system based upon our previous findings. Next, we chose (ii) *AM* as the therapeutic gene because of its reported effectiveness in the transient treatment of PAH. For the route of administration, we selected (iii) intratracheal administration to avoid the rapid propensity of nuclease degradation in the blood compartment and also that we might exploit the lung, based upon its enormous surface area, for

© The American Society of Gene Therapy

use as a therapeutic bioreactor for AM production. Pulmonary administration is a promising therapeutic route of administration in the clinic for its (iv) high patient compliance with utilization of an inhaler or nebulizer.

Recently, we have demonstrated that PEG-*b*-P[Asp(DET)] polyplex nanomicelles achieved amplified *in vitro* and *in vivo* transfection activity with minimal cytotoxicity.[14–16,21] With regard to the transfection mechanism, P[Asp(DET)] possesses the ethylenediamine side chain, which undergoes two-step protonation from the mono-protonated gauche form at physiological pH to di-protonated anti form at acidic pH, thereby exhibiting an effective buffering function in the acidic endosomal compartment.[22] Also, we revealed the membrane destabilization effect of P[Asp(DET)] responding to acidic endosomal pH conditions by hemolysis, leakage of cytoplasmic enzyme (lactate dehydrogenase assay), and confocal laser scanning microscopic observation.[22] Consequently, we observed the facilitated transport of Cy5-labeled plasmid DNA by the P[Asp(DET)] polyplexes from endo/lysosomal compartment into cytoplasm directly under the confocal laser scanning microscope in single cellular level.[22] Therefore, the increased transgene expression in **Figure 3** may be a result of the facilitated translocation of the polyplex nanomicelles from the endosome to the cytoplasm based on the buffering capacity (proton sponge effect) and/or endosomal membrane–destabilizing effect of P[Asp(DET)] segment. The reason why a relatively high N/P ratio was required for the efficient transfection (**Figure 3**) may be because the membrane-destabilizing effect of P[Asp(DET)] is dependent on the polymer concentration as previously reported. Nevertheless, the PEG-*b*-P[Asp(DET)] polyplex nanomicelles displayed minimal cytotoxicity even at a high N/P ratio, which may be due to the pH-sensitive properties of P[Asp(DET)] segment.[22] The highly transfectable but less cytotoxic properties of PEG-*b*-P[Asp(DET)] polyplex nanomicelles motivated us to apply them to the gene therapy of PAH animal models through the intratracheal administration in this study.

A number of nonviral vectors including polyplex and lipoplex have been applied for *in vivo* intratracheal transfection. Special notice for the pulmonary gene delivery via airways is that the lung has the features critically influencing the transfection efficiency, such as the presence of surfactant, alveolar macrophages, and mucocilliary clearance mechanisms. In the early 1990s, lipoplex was used by aerosol delivery or intratracheal instillation. However, cationic lipids were shown to have a decreased transfection efficiency due to the interaction with lung surfactant compared to cationic polymer like PEI.[23,24] To overcome the surfactant barriers, cationic emulsion was used and showed much higher transfection activity compared with lipoplexes, such as lipofectin, lipofectamine, and DMRIE/c.[25] However, even for the cationic emulsion, the luciferase activity was limited to 55 pg/mg protein, which is significantly lower than the value attained by the polyplex nanomicelles loaded with PEG-*b*-P[Asp(DET)] [3,000,000 relative light unit/mg protein (135 ng/mg protein)] as reported here. Polyplexes made from cationic polymer was reported to show higher transfection efficiency compared with cationic lipoplexes for pulmonary gene delivery via airways.[23,24] PEI or modified PEI has been shown to be one of the most effective agents for constructing gene delivery systems available today with high levels of pulmonary gene transfer by airways.[26,27] Intratracheal injection of polyplex loaded with 22 kd of LPEI (ExGen 500) showed up to 20,000–40,000 relative light unit/mg protein of luciferase activity in the lung by adjusting N/P ratio. Worth noting is that the nanomicelles achieved two orders of magnitude higher value in luciferase gene expression compared to the LPEI polyplex. Furthermore, no induction of cytokine responses is appealing for the nanomicelles over LPEI polyplex (**Figure 6**), which was reported to induce the activation of $CD8^+$ and $CD4^+$ T cells, and Fas ligand–mediated antigen-induced cell death.[28,29]

To ameliorate the symptoms of PAH in animal models, several genes have been identified including: endothelial nitric-oxide synthase, inducible nitric-oxide synthase, prostacyclin synthase, calcium gene-related peptide, vascular endothelial growth factor, and hepatocyte growth factor.[18–20,30–36] We used AM as a therapeutic gene because of its high potency and long-term effectiveness as a vasodilator in the pulmonary vascular bed.[37] The effect of pulmonary vasodilation is mediated by cyclic adenosine monophosphate–dependent and nitric oxide–dependent mechanisms.[38] PAH patients have elevated plasma AM concentrations, which increase in step with the disease's severity[39,40] often resulting in pulmonary hypotension. In previous studies, intravenous administration[41] and inhalation[8] of the AM peptide showed acute hemodynamic and hormonal efficacy in PAH patients. However, despite alternative routes of delivery, the small AM peptide was rapidly degraded *in vivo* displaying a poor pharmacokinetic profile with a temporal window of only 30–45 minutes. For the treatment of PAH, sustained effect of AM is required. In this report, the therapeutic indicator for successful nonviral AM delivery was a decrease in the right ventricular pressure. Indeed, for the polyplex nanomicelle/pAM formulation, the right ventricular pressure did decrease, but more importantly the persistence of *AM* gene expression continued within a therapeutic range for a minimum of 3 days. The results indicate that the therapeutic approach using the polyplex nanomicelle as a vector does not require chronic infusion or very frequent inhalation, which will make the therapy more clinically applicable.

In this study, we succeeded in delivering DNA to the lung via intratracheal administration using the polyplex nanomicelles, resulting in extremely improved transfection efficiency with concomitant high biocompatibility. More specifically, the lung transfected with the polyplex nanomicelle had much lower toxicity than that transfected with the LPEI polyplex, according to the histological findings and measurement of the mRNA levels of inflammatory cytokines (**Figure 6a–d**). We also developed an effective treatment for the PAH rat model by delivering the therapeutic *AM* gene with polyplex nanomicelles from PEG-*b*-P[Asp(DET)]. These results showed a significant increase in transfection efficiently *in vivo* with intratracheal administration. The PEG-*b*-P[Asp(DET)] polyplex nanomicelle delivery system clearly showed promising *in vivo* results of transgene and therapeutic AM expression, when coupled with the clear visual, localization of the polyplex nanomicelles in the pulmonary tissue and the lack of proinflammatory responses. We posit that the PEG-*b*-P[Asp(DET)] nonviral gene carrier clearly shows those characteristics requisite for novel and advanced therapeutic systems ideally suited for translational research.

© The American Society of Gene Therapy

MATERIALS AND METHODS

Materials. An expression vector for YFP (RIKEN, Tokyo, Japan) was amplified in competent HB101 *Escherichia coli* and purified by Plasmid Giga Kits (Qiagen, Hilden, Germany). An expression vector for luciferase with a CAG promoter was provided by RIKEN. An expression vector for human AM was constructed as follows. The *EcoRI/XhoI* fragment of the full-length human AM complementary DNA (cDNA)[42] was ligated into the *EcoRI/XhoI* site of pcDNA1 (Invitrogen, Carlsbad, CA). The restriction maps of expression vector for luciferase and human AM cDNA are listed in **Supplementary Figure S1a,b**, respectively. To confirm that pcDNA/AM encodes AM, pcDNA/AM was transfected into Chinese hamster ovary cells, and the medium and the cells were collected for the measurement of immunoreactive AM using an AM radioimmunoassay Shionogi (Cosmic, Tokyo, Japan).

Animals. Male ICR mice weighing 25–30 g were administered the reporter gene intratracheally. Male Wistar rats weighing 100–120 g were used to make a model of PAH. All protocols were performed in accordance with the guidelines of the Animal Care Ethics Committee of the National Cardiovascular Center Research Institute (Osaka, Japan).

Synthesis and characterization of PEG-b-P[Asp(DET)]. PEG-*b*-P[Asp(DET)] was prepared as previously described.[14] Briefly, PEG-poly(β-benzyl-L-aspartate) (PEG-PBLA) diblock copolymer was synthesized by the ring-opening polymerization of β-benzyl-L-aspartate *N*-carboxyanhydride from the terminal primary amino group of α-methoxy-ω-amino PEG (M_w: 12,000; Nippon Oil and Fats, Tokyo, Japan). Gel-permeation chromatography confirmed that the copolymer was unimodal with a narrow molecular weight distribution (M_w/M_n: 1.23), and the number of benzyl-L-aspartate repeating units was calculated to be 68 by ^{1}H-NMR. The N-terminal amino group of PEG-PBLA was then acetylated using acetic anhydride in dichloromethane solution to obtain PEG-PBLA-Ac. The obtained polymer was dissolved in distilled *N,N*-dimethylformamide (Wako Pure Chemical Industries, Osaka, Japan) and reacted with diethylenetriamine (Tokyo Kasei Kogyo, Tokyo, Japan) for 24 hours at 40 °C in a dry argon atmosphere to undergo aminolysis of the benzyl side chain. After 24 hours, the solution was slowly dripped into a 10% acetic acid solution and dialyzed (Spectra/Por Membrane, 3,500 molecular weight cutoff; Spectrum Laboratories, Rancho Dominguez, CA) against 0.01 N HCl and subsequently against distilled water. The final solution was lyophilized to obtain PEG-*b*-P[Asp(DET)] as the hydrochloride salt form. ^{1}H-NMR confirmed the complete substitution of benzyl ester of the polymer with diethylenetriamine through the aminolysis reaction, as well as the chemical structure of the obtained PEG-*b*-P[Asp(DET)] block copolymer.

Preparation of polyplex nanomicelles. The PEG-*b*-P[Asp(DET)] block copolymer and plasmid DNA were separately dissolved in 10 mmol/l HEPES buffer (pH 7.4). Both solutions were mixed at the indicated nitrogen/phosphate ratios [=(total amines in cationic segment)/(phosphates in plasmid DNA)] and incubated overnight at room temperature to make PEG-*b*-P[Asp-(DET)] polyplex nanomicelle. LPEI (ExGen; Cosmo Bio, Tokyo, Japan) polyplexes were prepared by mixing plasmid DNA and LPEI according to the manufacturer's protocol.

In vivo *gene delivery by intratracheal administration.* ICR mice were anesthetized by intraperitoneal administration of pentobarbital (30 mg/kg) (Dainippon Sumitomo Pharma, Osaka, Japan). Tracheostomies were performed under sterile conditions for PEG-*b*-P[Asp-(DET)] polyplex nanomicelle or LPEI polyplex (10 μg of DNA for each mouse) in a 50 μl of solution administration by a microsprayer Model IA-1C (Penn Century, Philadelphia, PA). After the indicated time, the mice were killed by cervical dislocation and the pulmonary tissues harvested. To measure luciferase activity, the pulmonary tissues were homogenized in a lysis buffer using a polytron. The lysate was then centrifuged at 14,000*g* for 10 minutes at 4 °C, and 20 μl of the supernatant was analyzed for luciferase activity by a Luminous CT-9000D luminometer (Dia-Iatron, Tokyo, Japan), according to a previously described method.[43] Background of luciferase activity in the lung was measured from the lung of mice after administration of saline, which was <3% of the total activity of day 14. All the data of luciferase activity were obtained by subtraction of background data. To detect YFP expression, mice were killed by cervical dislocation and the lungs harvested. Frozen sections (5-μm thick) of the lung specimens were visualized by a fluorescence microscope (SZX12; Olympus, Tokyo, Japan). To examine the histological features of the lung tissue, the specimens were also fixed in 4% paraformaldehyde and embedded in paraffin. Sections (3-μm thick) were stained with hematoxylin.

Isolation of RNA and cDNA synthesis. Total RNA was extracted using the Trizol method (Gibco BRL Life Technologies, Breda, Netherlands) according to the protocol provided by the manufacturer. The RNA was dissolved in RNAse-free water and quantified by a spectrophotometer. The cDNA was synthesized using the High Capacity cDNA Reverse Transcription Kit (Applied Biosystems, Foster City, CA).

Real-time RT-PCR. mRNA expression levels of TNF-α, IL-6, IL-10, Cox-2 and human AM were measured by quantitative real-time RT-PCR based on TaqMan chemistry (Applied Biosystems) using an ABI PRISM 7700 sequence detector (Applied Biosystems). The reaction mixture contained 0.5 μl of 5 μmol/l probe (final concentration, 100 nmol/l); 1 μl of 10 μmol/l forward primer and 1 μl of 10 μmol/l reverse primer (400 nmol/l final concentration of each primer); 12.5 μl of TaqMan Universal Mastermix, 5 μl of diethyl pyrocarbonate–treated water, and 5 μl of a cDNA sample. Assay controls were performed in the same TaqMan plate with no-template controls to test for the contamination of any assay reagents. The thermocycling conditions were initiated at 50 °C for 2 minutes with an enzyme activation step of 95 °C for 10 minutes followed by 40 PCR cycles of denaturation at 95 °C for 15 seconds, and anneal/extension at 60 °C for 1 minute.

Hemodynamic studies. Hemodynamic studies were performed 4 weeks after gene transfer. Rats were anesthetized with intraperitoneal pentobarbital (30 mg/kg) and placed on a heating pad to maintain body temperature 37–38 °C throughout the study. Under sterile conditions, a polyethylene catheter (PE-50; BD Biosciences, San Jose, CA) was inserted through the right jugular vein into the right ventricle to measure right ventricular pressure by a hemodynamic transducer (PowerLab 8/30; ADInstruments, Colorado Springs, CO).

Evaluation of gene transfer effect in a PAH rat model. Monocrotaline (60 mg/kg) was subcutaneously injected into male Wistar rats and left for 4 weeks to make a model of PAH. After 4 weeks, a hemodynamic study was performed to introduce a catheter into the right ventricle through the right jugular vein. The PEG-*b*-P[Asp(DET)] polyplex nanomicelle loaded with the AM expression vector (200 μg of DNA for each rat) in a 200 μl of solution was sprayed intratracheally. Three days later, a hemodynamic study was performed again and the gene transfer effect was evaluated. Pulmonary tissue specimens were frozen to measure *AM* gene expression by real-time RT-PCR.

Statistical analysis. All data are expressed as means ± SEM unless otherwise indicated. Comparisons of parameters among four groups were made by one-way analysis of variance, followed by Scheffe's multiple-comparison test. Paired *t*-test was applied for the comparison of the values before and after the gene transfection (**Figure 7**).

SUPPLEMENTARY MATERIAL

Figure S1. The restriction maps of expression vector for luciferase and human adrenomedullin cDNA.

ACKNOWLEDGMENTS

This work was supported by the Core Research Program for Evolutional Science and Technology from the Japan Science and Technology

© The American Society of Gene Therapy

Corporation, by Grants-in-Aid for Scientific Research from the Japanese Ministry of Health, Labor, and Welfare (H19-Nano-012 and H20-Genomu-Ippan-008), by the Program for the Promotion of Fundamental Studies in Health Sciences of the National Institute of Biomedical Innovation of Japan, and by the Takeda Science Foundation. We thank Keiko Jinno, Shoko Obora, Hiroko Miyata, Moto Ohira, and Eri Abe and Mutsumi Goda (National Cardiovascular Center Research Institute) for their excellent technical assistance, including animal care. We also thank Hisayuki Matsuo and Hitonobu Tomoike for their helpful discussion and advice, Darin Y. Furgeson (University of Wisconsin–Madison) for proofreading of this manuscript.

REFERENCES

1. Rubin, LJ (2006). Pulmonary arterial hypertension. *Proc Am Thorac Soc* **3**: 111–115.
2. Badesch, DB, Abman, SH, Ahearn, GS, Barst, RJ, McCrory, DC, Simonneau, G *et al.* (2004). Medical therapy for pulmonary arterial hypertension: ACCP evidence-based clinical practice guidelines. *Chest* **126**(1 Suppl): 35S–62S.
3. D'Alonzo, GE, Barst, RJ, Ayres, SM, Bergofsky, EH, Brundage, BH, Detre, KM *et al.* (1991). Survival in patients with primary pulmonary hypertension. Results from a national prospective registry. *Ann Intern Med* **115**: 343–349.
4. Kitamura, K, Kangawa, K, Kawamoto, M, Ichiki, Y, Nakamura, S, Matsuo, H *et al.* (1993). Adrenomedullin: a novel hypotensive peptide isolated from human pheochromocytoma. *Biochem Biophys Res Commun* **192**: 553–560.
5. Kitamura, K, Kangawa, K and Eto, T (2002). Adrenomedullin and PAMP: discovery, structures, and cardiovascular functions. *Microsc Res Tech* **57**: 3–13.
6. Nagaya, N, Mori, H, Murakami, S, Kangawa, K and Kitamura, S (2005). Adrenomedullin: angiogenesis and gene therapy. *Am J Physiol Regul Integr Comp Physiol* **288**: R1432–R1437.
7. Nagaya, N, Okumura, H, Uematsu, M, Shimizu, W, Ono, F, Shirai, M *et al.* (2003). Repeated inhalation of adrenomedullin ameliorates pulmonary hypertension and survival in monocrotaline rats. *Am J Physiol Heart Circ Physiol* **285**: H2125–H2131.
8. Nagaya, N, Kyotani, S, Uematsu, M, Ueno, K, Oya, H, Nakanishi, N *et al.* (2004). Effects of adrenomedullin inhalation on hemodynamics and exercise capacity in patients with idiopathic pulmonary arterial hypertension. *Circulation* **109**: 351–356.
9. Katayose, S and Kataoka, K (1997). Water-soluble polyion complex associates of DNA and poly(ethylene glycol)-poly(L-lysine) block copolymer. *Bioconjug Chem* **8**: 702–707.
10. Kakizawa, Y and Kataoka, K (2002). Block copolymer micelles for delivery of gene and related compounds. *Adv Drug Deliv Rev* **54**: 203–222.
11. Katayose, S and Kataoka, K (1998). Remarkable increase in nuclease resistance of plasmid DNA through supramolecular assembly with poly(ethylene glycol)-poly(L-lysine) block copolymer. *J Pharm Sci* **87**: 160–163.
12. Itaka, K, Yamauchi, K, Harada, A, Nakamura, K, Kawaguchi, H and Kataoka, K (2003). Polyion complex micelles from plasmid DNA and poly(ethylene glycol)-poly(L-lysine) block copolymer as serum-tolerable polyplex system: physicochemical properties of micelles relevant to gene transfection efficiency. *Biomaterials* **24**: 4495–4506.
13. Harada-Shiba, M, Yamauchi, K, Harada, A, Takamisawa, I, Shimokado, K and Kataoka, K (2002). Polyion complex micelles as vectors in gene therapy—pharmacokinetics and *in vivo* gene transfer. *Gene Ther* **9**: 407–414.
14. Kanayama, N, Fukushima, S, Nishiyama, N, Itaka, K, Jang, WD, Miyata, K *et al.* (2006). A PEG-based biocompatible block catiomer with high buffering capacity for the construction of polyplex micelles showing efficient gene transfer toward primary cells. *ChemMedChem* **1**: 439–444.
15. Itaka, K, Ohba, S, Miyata, K, Kawaguchi, H, Nakamura, K, Takato, T *et al.* (2007). Bone regeneration by regulated *in vivo* gene transfer using biocompatible polyplex nanomicelles. *Mol Ther* **15**: 1655–1662.
16. Akagi, D, Oba, M, Koyama, H, Nishiyama, N, Fukushima, S, Miyata, T *et al.* (2007). Biocompatible micellar nanovectors achieve efficient gene transfer to vascular lesions without cytotoxicity and thrombus formation. *Gene Ther* **14**: 1029–1038.
17. Nossaman, BD, Gur, S and Kadowitz, PJ (2007). Gene and stem cell therapy in the treatment of erectile dysfunction and pulmonary hypertension; potential treatments for the common problem of endothelial dysfunction. *Curr Gene Ther* **7**: 131–153.
18. Champion, HC, Bivalacqua, TJ, Greenberg, SS, Giles, TD, Hyman, AL, Kadowitz, PJ (2002). Adenoviral gene transfer of endothelial nitric-oxide synthase (eNOS) partially restores normal pulmonary arterial pressure in eNOS-deficient mice. *Proc Natl Acad Sci USA* **99**: 13248–13253.
19. Champion, HC, Bivalacqua, TJ, Toyoda, K, Heistad, DD, Hyman, AL and Kadowitz, PJ (2000). *In vivo* gene transfer of prepro-calcitonin gene-related peptide to the lung attenuates chronic hypoxia-induced pulmonary hypertension in the mouse. *Circulation* **101**: 923–930.
20. Nagaya, N, Yokoyama, C, Kyotani, S, Shimonishi, M, Morishita, R, Uematsu, M *et al.* (2000). Gene transfer of human prostacyclin synthase ameliorates monocrotaline-induced pulmonary hypertension in rats. *Circulation* **102**: 2005–2010.
21. Masago, K, Itaka, K, Nishiyama, N, Chung, UI and Kataoka, K (2007). Gene delivery with biocompatible cationic polymer: Pharmacogenomic analysis on cell bioactivity. *Biomaterials* **28**: 5169–5175.
22. Miyata, K, Oba, M, Nakanishi, M, Fukushima, S, Yamasaki, Y, Koyama, H *et al.* (2008). Polyplexes from poly(aspartamide) bearing 1,2-diaminoethane side chains induce pH-selective, endosomal membrane destabilization with amplified transfection and negligible cytotoxicity. *J Am Chem Soc* **130**: 16287–16294.
23. Bragonzi, A, Dina, G, Villa, A, Calori, G, Biffi, A, Bordignon, C *et al.* (2000). Biodistribution and transgene expression with nonviral cationic vector/DNA complexes in the lungs. *Gene Ther* **7**: 1753–1760.
24. Wiseman, JW, Goddard, CA, McLelland, D and Colledge, WH (2003). A comparison of linear and branched polyethylenimine (PEI) with DCChol/DOPE liposomes for gene delivery to epithelial cells *in vitro* and *in vivo*. *Gene Ther* **10**: 1654–1662.
25. Kim, TW, Chung, H, Kwon, IC, Sung, HC, Shin, BC and Jeong, SY (2005). Airway gene transfer using cationic emulsion as a mucosal gene carrier. *J Gene Med* **7**: 749–758.
26. Densmore, CL (2006). Advances in noninvasive pulmonary gene therapy. *Curr Drug Deliv* **3**: 55–63.
27. Furgeson, DY, Chan, WS, Yockman, JW and Kim, SW (2003). Modified linear polyethylenimine-cholesterol conjugates for DNA complexation. *Bioconjug Chem* **14**: 840–847.
28. Gautam, A, Densmore, CL and Waldrep, JC (2001). Pulmonary cytokine responses associated with PEI-DNA aerosol gene therapy. *Gene Ther* **8**: 254–257.
29. Regnstrom, K, Ragnarsson, EG, Koping-Hoggard, M, Torstensson, E, Nyblom, H and Artursson, P (2003). PEI—a potent, but not harmless, mucosal immuno-stimulator of mixed T-helper cell response and FasL-mediated cell death in mice. *Gene Ther* **10**: 1575–1583.
30. Budts, W, Pokreisz, P, Nong, Z, Van Pelt, N, Gillijns, H, Gerard, R *et al.* (2000). Aerosol gene transfer with inducible nitric oxide synthase reduces hypoxic pulmonary hypertension and pulmonary vascular remodeling in rats. *Circulation* **102**: 2880–2885.
31. Chicoine, LG, Tzeng, E, Bryan, R, Saenz, S, Paffett, ML, Jones, J *et al.* (2004). Intratracheal adenoviral-mediated delivery of iNOS decreases pulmonary vasoconstrictor responses in rats. *J Appl Physiol* **97**: 1814–1822.
32. Campbell, AI, Zhao, Y, Sandhu, R and Stewart, DJ (2001). Cell-based gene transfer of vascular endothelial growth factor attenuates monocrotaline-induced pulmonary hypertension. *Circulation* **104**: 2242–2248.
33. Gong, F, Tang, H, Lin, Y, Gu, W, Wang, W and Kang, M (2005). Gene transfer of vascular endothelial growth factor reduces bleomycin-induced pulmonary hypertension in immature rabbits. *Pediatr Int* **47**: 242–247.
34. Suhara, H, Sawa, Y, Fukushima, N, Kagisaki, K, Yokoyama, C, Tanabe, T *et al.* (2002). Gene transfer of human prostacyclin synthase into the liver is effective for the treatment of pulmonary hypertension in rats. *J Thorac Cardiovasc Surg* **123**: 855–861.
35. Ono, M, Sawa, Y, Fukushima, N, Suhara, H, Nakamura, T, Yokoyama, C *et al.* (2004). Gene transfer of hepatocyte growth factor with prostacyclin synthase in severe pulmonary hypertension of rats. *Eur J Cardiothorac Surg* **26**: 1092–1097.
36. Ono, M, Sawa, Y, Mizuno, S, Fukushima, N, Ichikawa, H, Bessho, K *et al.* (2004). Hepatocyte growth factor suppresses vascular medial hyperplasia and matrix accumulation in advanced pulmonary hypertension of rats. *Circulation* **110**: 2896–2902.
37. Lippton, H, Chang, JK, Hao, Q, Summer, W and Hyman, AL (1994). Adrenomedullin dilates the pulmonary vascular bed *in vivo*. *J Appl Physiol* **76**: 2154–2156.
38. Ishizaka, Y, Ishizaka, Y, Tanaka, M, Kitamura, K, Kangawa, K, Minamino, N *et al.* (1994). Adrenomedullin stimulates cyclic AMP formation in rat vascular smooth muscle cells. *Biochem Biophys Res Commun* **200**: 642–646.
39. Kakishita, M, Nishikimi, T, Okano, Y, Satoh, T, Kyotani, S, Nagaya, N *et al.* (1999). Increased plasma levels of adrenomedullin in patients with pulmonary hypertension. *Clin Sci (Lond)* **96**: 33–39.
40. Yoshibayashi, M, Kamiya, T, Kitamura, K, Saito, Y, Kangawa, K, Nishikimi, T *et al.* (1997). Plasma levels of adrenomedullin in primary and secondary pulmonary hypertension in patients <20 years of age. *Am J Cardiol* **79**: 1556–1558.
41. Nagaya, N, Nishikimi, T, Uematsu, M, Satoh, T, Oya, H, Kyotani, S *et al.* (2000). Haemodynamic and hormonal effects of adrenomedullin in patients with pulmonary hypertension. *Heart* **84**: 653–658.
42. Kitamura, K, Sakata, J, Kangawa, K, Kojima, M, Matsuo, H and Eto, T (1993). Cloning and characterization of cDNA encoding a precursor for human adrenomedullin. *Biochem Biophys Res Commun* **194**: 720–725.
43. de Wet, JR, Wood, KV, DeLuca, M, Helinski, DR and Subramani, S (1987). Firefly luciferase gene: structure and expression in mammalian cells. *Mol Cell Biol* **7**: 725–737.

Atherosclerosis 204 (2009) 590–594

Contents lists available at ScienceDirect

Atherosclerosis

journal homepage: www.elsevier.com/locate/atherosclerosis

Plasma des-acyl ghrelin, but not plasma HMW adiponectin, is a useful cardiometabolic marker for predicting atherosclerosis in elderly hypertensive patients

Yuichiro Yano[a,b,*], Koji Toshinai[c], Takashi Inokuchi[d], Kenji Kangawa[e], Kazuyuki Shimada[b], Kazuomi Kario[b], Masamitsu Nakazato[c]

[a] Division of Internal Medicine, Nango National Health Insurance Hospital, Japan
[b] Division of Cardiovascular Medicine, Department of Medicine, Jichi Medical University School of Medicine, Japan
[c] Division of Neurology, Respirology, Endocrinology and Metabolism, Department of Internal Medicine, Miyazaki Medical College, University of Miyazaki, Japan
[d] Department of Orthopedic Surgery, Kitaura National Health Insurance Hospital, Japan
[e] Department of Biochemistry, National Cardiovascular Center Research Institute, Japan

ARTICLE INFO

Article history:
Received 9 August 2008
Received in revised form
17 September 2008
Accepted 12 October 2008
Available online 1 November 2008

Keywords:
Des-acyl ghrelin
HMW adiponectin
Obesity
Elderly
Atherosclerosis

ABSTRACT

Objective: The coming obesity epidemic in elderly persons necessitates the establishment of new and easy-to-use cardiometabolic markers to identify individuals most likely to develop atherosclerosis among hypertensives.
Methods: We measured plasma HMW adiponectin and des-acyl ghrelin levels, and carotid-artery intima-media thickness (cIMT) in 263 elderly hypertensives (mean 72.6 years; 37%men). Other cardiometabolic markers, including metabolites, inflammation, and hemostasis, were also measured.
Results and conclusion: Both HMW adiponectin and des-acyl ghrelin levels were inversely correlated with obesity. The HMW adiponectin level was favorably associated with glucose and lipid metabolites, PAI-1 (all $P<0.05$), and hs-CRP ($P=0.07$) after adjustment for age, sex, and BMI; however, it had no correlations with cIMT. In contrast, although there were no correlations between des-acyl ghrelin and cardiometabolic markers, except for a positive association with the nitrite/nitrate (NO_x) level ($P=0.002$), des-acyl ghrelin had a significant inverse correlation with cIMT ($P=0.003$). A multivariable regression analysis showed that des-acyl ghrelin, but not HMW adiponectin, was significantly associated with cIMT after adjusting for age, obesity, sex, smoking, 24-h BP, and other cardiometabolic factors ($\beta=-0.178$, $P=0.001$). Moreover, the increased risk of cIMT among those with abdominal obesity compared with non-obesity (0.833 ± 0.185 mm vs. 0.782 ± 0.163 mm, $P=0.019$) was explained by the elevated 24-h BP and reduced des-acyl ghrelin level, but not by other cardiometabolic parameters. These associations were unchanged after adding NO_x to the model. In conclusion, the des-acyl ghrelin level is a useful cardiometabolic marker for predicting atherosclerosis in elderly hypertensives, and the pathologic pathway linking these factors is independent of its NO bioactivity.

© 2008 Elsevier Ireland Ltd. All rights reserved.

1. Introduction

Due to the growing obesity epidemic and the growing elderly population, it is essential that we improve our understanding of the impact of obesity on the cardiovascular system in elderly persons, and establish new and easy-to-use cardiometabolic markers to identify individuals most likely to develop atherosclerosis among hypertensives [1]. A recent study has revealed that endocrine functions (i.e., adipocytokines) are involved in the pathophysiological mechanisms underlying the risk factors associated with obesity and atherosclerosis [2], but the roles of adipocytokines in these mechanisms are only partially understood.

Adiponectin, an adipocyte-derived hormone, has favorable effects on insulin-sensitizing, anti-inflammatory, and anti-atherogenic properties [3], and thus high adiponectin levels have been associated with a reduction of cardiovascular disease (CVD) [3,4]. However, recent prospective studies have shown conflicting results, particularly in elderly persons [5], suggesting that adiponectin may have different clinical implications in the elderly. High adiponectin in the elderly is a consequence of weight loss

* Corresponding author at: Division of Internal Medicine, Nango National Health Insurance Hospital, 1078 Mikado, Nango, Misato Town, Miyazaki 883-0306, Japan. Tel.: +81 982 59 0017; fax: +81 982 59 0213.
E-mail address: yyano@jichi.jp (Y. Yano).

0021-9150/$ – see front matter © 2008 Elsevier Ireland Ltd. All rights reserved.
doi:10.1016/j.atherosclerosis.2008.10.013

and sarcopenia with aging [5–7], both of which are predictors of mortality [8]. In addition, adiponectin could exert its own effects by increasing energy expenditures and thereby leading to wasting [7]. Recently, increasing attention has been paid to the multimeric isoforms of adiponectin. In the circulation, adiponectin exists in at least three multimeric isoforms: a low-, medium- and high-molecular-weight (HMW) form. These different oligomeric forms of adiponectin might activate different signaling pathways and exert distinct functions on its target tissues. Because HMW adiponectin may be the major active form of the metabolic and vascular protective effects of adiponectin [3,6,9], it would be worthwhile to examine its clinical implications in elderly persons.

In contrast, ghrelin, an endogenous ligand for the growth hormone secretagogue receptor (GHSR) and acts as an anabolic hormone in elderly persons [10,11], has been shown to exert not only energy homeostasis, but also cardiometabolic regulations in both healthy and obese subjects [12,13]. The reduction of ghrelin, which is associated with obesity, has also been shown to be proportional to aging and catabolic rates, and thus it may be more representative of a true biological phenomenon in elderly persons. Des-acyl ghrelin, a more abundant form of ghrelin in humans and allows easier measurement than acylated ghrelin, has some unique cardiometabolic properties, such as blood pressure (BP) lowering [12], nitric oxide (NO) production [13], and prevention of cardiac and endothelial cell apoptosis [14]. However, there have been no studies examining these effects in humans.

In the present study, we measured plasma HMW adiponectin and des-acyl ghrelin levels, and examined their relationship to obesity-related cardiometabolic factors, including glucose and lipid metabolism, inflammation (high-sensitivity C-reactive protein: hsCRP), hemostasis (plasminogen activator inhibitor-1: PAI-1), and atherosclerosis (carotid artery intima-media thickness: cIMT) in elderly hypertensives.

2. Subjects and methods

276 consecutive ambulatory patients with essential hypertension who were >40 years old and who had been referred to our outpatient clinic (Kitaura National Health Insurance Hospital, Miyazaki, Japan) were recruited for the Miyazaki Elderly-Fat (EL-FAT) project (see Supplementary materials). The project was approved by the institutional review board at Jichi Medical University, and written informed consent was obtained from all the participants. All patients completed a health questionnaire and provided their complete medical history (smoking and drinking status, physical activity, use of medications, and past medical history), and underwent measurement of body mass index (BMI) and waist circumference (WC), office and 24-h ambulatory BP monitoring (ABPM), blood sampling, and carotid ultrasonography. Hypertension was defined as use of anti-hypertensive drugs or an office BP level of ≥140/90 mmHg. Type 2 diabetes was defined as use of anti-hyperglycemic drugs or a fasting glucose of ≥126 mg/dl. The exclusion criteria were as follows: a history of coronary arterial disease (CAD), cerebrovascular disease, or heart failure in the past 3 months; presence of inflammatory diseases (acute infection, autoimmune diseases); presence of malignant diseases; presence of gastrectomy; and absence of or incomplete sampling data.

2.1. Laboratory testing

To measure the des-acyl ghrelin level, a fasting venous sample was carefully collected via a 21-gauge needle into a syringe containing EDTA-2Na (1.25 mg/ml) and aprotinin (Ohkura Pharmaceutical, Inc., Kyoto, Japan; 500 kallikrein inactivator U/ml) at 08:00–08:30 h. Plasma was obtained by centrifuging the whole blood at 1500 × *g* for 15 min at 4 °C, and was immediately frozen and stored at −40 °C until analysis. We used a commercially available ELISA Kit (Mitsubishi Kagaku Iatron Co., Tokyo, Japan) [15]. HMW adiponectin concentrations were measured using a two-step sandwich ELISA system (FujiRevio Inc., Tokyo, Japan), and the levels of nitrite/nitrate (NO_x) (NO_2^- and NO_3^-) in serum were measured using a high-performance liquid chromatography ultraviolet (HPLC-UV) system. Methods of other parameters are described in detail in the Supplementary materials. The intraassay and interassay coefficients of laboratory tests were all <7%.

2.2. ABPM and carotid ultrasonography

For full details, see the Supplementary materials. Briefly, as described in a previous report [16], cIMT was calculated by averaging the values from three different sites on each common carotid artery: the point of greatest thickness, and points 1 cm upstream and 1 cm downstream from the point of greatest thickness. The average of the right and left cIMT was defined as the mean cIMT.

2.3. Statistical analysis

All statistical analyses were performed with SPSS version 16.0J software (SPSS, Chicago, IL). Data are expressed as the means ± S.D. or median (25th to 75th percentile). The associations between the individual parameters were calculated using Spearman's correlation method. To identify factors associated with the development of cIMT, we used a step-wise multivariable linear regression analysis in which a *P*-value of 0.05 or less in a simple regression analysis was used as the criterion for entry into the model. Variables with skewed distribution were logarithmically transformed before analysis. We also used the κ^2 test for categorical analysis and unpaired *t*-test to compare differences between subjects with or without abdominal obesity, and the difference in cIMT was assessed using ANOVA with post hoc Bonferroni corrections. Statistical significance was defined as $P<0.05$.

3. Results

3.1. Characteristics of the study population

Two patients who refused to participate, seven patients with incomplete ABPM, and four patients with unsatisfactory blood sampling were excluded. The characteristics of the remaining 263 subjects are shown in Table 1.

3.2. Association of HMW adiponectin with cardiometabolic markers

The plasma HMW adiponectin level was inversely correlated with BMI ($r=-0.215$, $P<0.001$), WC ($r=-0.253$, $P<0.001$), ever smoker ($r=-0.203$, $P<0.001$), GFR ($r=-0.305$, $P<0.001$), and diabetes ($r=-0.255$, $P<0.001$), and positively correlated with age ($r=0.353$, $P<0.001$) and female gender ($r=0.185$, $P<0.001$); however, the significant correlations between HMW adiponectin and BMI and WC disappeared with aging (≥75 years; $n=118$). The age-, sex-, and BMI-adjusted partial correlations between HMW adiponectin and cardiometabolic markers are shown in Table 2. Additional adjustments for medications, including anti-hypertensive and lipid-lowering drugs, did not alter the associations (data not shown).

Table 1
Characteristics of the study population.

	Total subjects (n = 263)
Age (years)	72.6 ± 8.4
Men, n (%)	96 (37)
BMI (kg/m^2)	24.4 ± 3.5
Waist, cm	86.0 ± 9.5
Ever smoker, n (%)	89 (34)
Anti-hypertensive medications, n (%)	214 (81)
Type 2 diabetes, n (%)	55 (21)
Stain, n (%)	62 (24)
CAD, n (%)	16 (6)
Cerebrovascular diseases, n (%)	25 (10)
GFR	69.6 ± 24.2
ABP measurement	
24-h SBP (mmHg)	134.9 ± 15.4
24-h DBP (mmHg)	77.7 ± 7.8
24-h HR (bpm)	67.2 ± 7.6
Laboratory testing	
Fasting glucose (mg/dl)	99.0 (91.0–112.0)
Insulin (μIU/ml)	5.7 (3.8–8.2)
High-density lipoprotein (mg/dl)	52.0 (44.0–61.0)
Triglycerides (mg/dl)	97.0 (71.0–131.0)
Low-density lipoprotein (mg/dl)	109.0 (91.0–132.0)
hs-CRP (mg/l)	0.58 (0.29–1.09)
PAI-1 (ng/ml)	34.0 (29.0–46.0)
IGF-1 (ng/ml)	103.0 (82.0–130.0)
NO_x (μmol/l)	32.0 (23.0–50.0)
HMW adiponectin (μg/ml)	7.0 (4.2–10.3)
Des-acyl ghrelin (fmol/ml)	108.7 (99.1–159.3)

Data are expressed as means ± S.D. or median (25th to 75th percentile). IGF-1: insulin-like growth factor-1.

3.3. Association of des-acyl ghrelin with cardiometabolic markers

The plasma des-acyl ghrelin level was inversely correlated with BMI (r = −0.155, P = 0.012) and WC (r = −0.162, P = 0.008), but showed no correlation with age, sex, smoking and drinking status, physical activity, or use of any drugs (all P = NS). Intriguingly, stronger inverse correlations between des-acyl ghrelin and BMI (r = −0.256, P = 0.005) and between des-acyl ghrelin and WC (r = −0.323, P < 0.001) were evident with aging (≥75 years). There were no correlations between plasma des-acyl ghrelin and any of the cardiometabolic markers, with the exception of the NO_x level, which showed a positive correlation with the des-acyl ghrelin level (Table 2).

3.4. Determinants of cIMT in elderly hypertensives

Table 3 shows the relation between the cIMT value and patients characteristics, and cardiometabolic markers. In a step-wise multivariate regression analysis including these significant covariates, age, smoking status, 24-h SBP, and the des-acyl ghrelin level remained independently correlated with the cIMT value (Table 4).

Table 2
Age-, sex-, and BMI-adjusted partial correlation among biomarkers.

	HMW adiponectin	Des-acyl ghrelin
Insulin	−0.364 (P < 0.001)	−0.064 (P = 0.301)
High-density lipoprotein	0.191 (P = 0.002)	0.036 (P = 0.560)
Triglycerides	−0.196 (P = 0.002)	0.014 (P = 0.821)
hs-CRP	−0.113 (P = 0.070)	0.076 (P = 0.220)
PAI-1	−0.148 (P = 0.017)	0.041 (P = 0.507)
IGF-1	0.034 (P = 0.585)	0.030 (P = 0.632)
NO_x	−0.009 (P = 0.886)	0.190 (P = 0.002)
HMW adiponectin	–	0.051 (P = 0.415)
Des-acyl ghrelin	0.051 (P = 0.415)	–

Statistical significance was defined as P < 0.05.

Table 3
Univariate analyses with cIMT in elderly hypertensives.

Variable	Spearman's correlation coefficient	P value
Age	0.407	<0.001
Sex (0 = men, 1 = women)	−0.125	0.044
Ever smoker (0 = No, 1 = Yes)	0.150	0.015
BMI	0.051	0.406
Waist	0.109	0.078
24-h SBP	0.259	<0.001
24-h DBP	−0.059	0.340
Insulin	−0.021	0.729
High-density lipoprotein	−0.117	0.059
Low-density lipoprotein	0.060	0.336
GFR	−0.262	<0.001
hs-CRP	−0.046	0.453
PAI-1	−0.122	0.048
IGF-1	−0.110	0.075
NO_x	0.051	0.419
HMW adiponectin	0.122	0.049
Des-acyl ghrelin	−0.180	0.003

Statistical significance was defined as P < 0.05.

Table 4
Multivariate analyses for determination of cIMT in elderly hypertensives.

Variable	Multivariate regression analysis*		
	$\beta^\dagger$	β (95% CI)	P value
Age	0.387	0.004 (0.003–0.005)	<0.001
Sex (0 = men, 1 = women)	0.021	–	0.785
Ever smoker (0 = No, 1 = Yes)	0.184	0.035 (0.015–0.056)	0.001
24-h SBP	0.212	0.001 (0.001–0.002)	<0.001
GFR	0.033	–	0.676
PAI-1	−0.101	–	0.068
HMW adiponectin	−0.010	–	0.863
Des-acyl ghrelin	−0.178	−0.061 (−0.097–−0.025)	0.001

$\beta^\dagger$: standardized coefficient; CI: confidence interval. Statistical significance was defined as P < 0.05.

* Variables with a P-value of 0.05 or less in a simple regression analysis with cIMT were used. Model summary: R^2 = 0.270, P < 0.001.

When NO_x was added to the model, the results were unchanged (data not shown). The significance of these explanatory variables was confirmed by dividing the population into two groups, those with cIMT above or below the median level (see Supplementary materials, Table S1). In addition, receiver–operator curves (ROC) were built to assess the power of biomarkers to predict a high cIMT level. In this way, des-acyl ghrelin was shown to be the best predictor (see Supplementary materials, Figure S1).

3.5. Effects of abdominal obesity and des-acyl ghrelin on atherosclerosis

We divided the subjects into two groups according to the presence of abdominal obesity (defined as WC ≥85 cm in men and ≥90 cm in women) [17]. cIMT was more elevated among those with abdominal obesity than in those without it (Table 5), which difference persisted even after adjustment for sex, smoking, insulin, triglycerides, hs-CRP, PAI-1, and HMW adiponectin (P = 0.022). However, this association was no longer significant after adding 24-h SBP (P = 0.151) or des-acyl ghrelin (P = 0.061) to the model. When added NO_x added to the model, the result was unchanged (data not shown).

4. Discussion

Our data indicate that although reductions of both plasma des-acyl ghrelin and plasma HMW adiponectin are associated with obesity, only the former is a useful cardiometabolic marker for pre-

Table 5
Anthropometric, hemodynamic, and cardiometabolic parameters in elderly hypertensives with or without abdominal obesity.

	Total subjects (n = 263)		P value
	Non-obesity (n = 136)	Abdominal obesity (n = 127)	
Age (years)	73.3 ± 8.2	71.9 ± 8.7	0.153
Men, n (%)	35 (26)	61 (48)	<0.001
BMI (kg/m^2)	22.3 ± 2.3	26.6 ± 3.1	<0.001
Waist (cm)	79.3 ± 6.1	93.1 ± 7.0	<0.001
A BP measurement			
24-h SBP (mmHg)	131.8 ± 12.7	138.3 ± 17.2	0.001
24-h DBP (mmHg)	76.5 ± 7.1	78.9 ± 8.3	0.010
Laboratory testing			
Insulin (μIU/ml)	4.8 (3.2–6.6)	6.9 (5.1–10.6)	<0.001
Triglycerides (mg/dl)	88.0 (68.0–119.8)	107.0 (79.0–154.0)	<0.001
hs-CRP (mg/l)	0.44 (0.21–0.93)	0.66 (0.36–1.28)	0.004
PAI-1 (ng/ml)	32.0 (27.0–40.0)	38.0 (30.0–54.0)	0.001
NO_x (μmol/l)	33.0 (23.0–50.0)	31.0 (23.0–51.0)	0.974
HMW adiponectin (μg/ml)	7.8 (5.0–11.3)	5.2 (3.5–8.9)	<0.001
Des-acyl ghrelin (fmol/ml)	116.8 (81.4–193.9)	98.3 (70.7–140.5)	0.003
cIMT (mm)	0.782 ± 0.163	0.833 ± 0.185	0.019

Data are expressed as means ± S.D. or median (25th to 75th percentile). Statistical significance was defined as $P < 0.05$.

dicting atherosclerosis in elderly hypertensives. Although there was a significant association between the des-acyl ghrelin and NO_x levels, the association of des-acyl ghrelin with atherosclerosis appears to be independent of the NO_x level. Because of previous experimental studies in which the cardiovascular protective effect of des-acyl ghrelin was suggested to be robust [12–14], the hypothesis that des-acyl ghrelin protects against the development of atherosclerosis is attractive. Our data warrant further investigation of the pathologic mechanisms responsible for this phenomenon and to clarify the prognostic value of this peptide with respect to cardiovascular events in the future.

4.1. Effects of HMW adiponectin on atherosclerosis in elderly hypertensives

Although the cardiovascular risks of obesity in elderly persons are still debatable [1,7], our data showed that elderly persons with abdominal obesity had a significantly higher level of cIMT. The mechanisms of this relation were not explained by the HMW adiponectin level or its related cardiometabolic parameters (glucose and lipid metabolites, inflammation, and hemostasis), despite the fact that the absolute magnitude of their difference between those with and without abdominal obesity was larger than for the des-acyl ghrelin level. Furthermore, the HMW adiponectin level could not predict the higher level of cIMT. These observations raised at least two possibilities. First, the detrimental effects of these parameters on atherosclerosis are generally weaker in elderly than middle-aged persons [1,5,8], which may be partially explained by the survival-effects [18]. Second, because HMW adiponectin could be influenced by many physiological and pathophysiological factors, interpretation of the HMW adiponectin level in elderly persons should be undertaken with caution. In fact, our study showed that the significant inverse association between HMW adiponectin and obesity [3–5] becomes attenuated with aging (≥75 years). This may be partly explained by the fact that the HMW adiponectin level is proportionally increased with age and impaired renal function, and thus an individual difference in advanced aging might become inconspicuous. Furthermore, our data show a significant inverse correlation between weight change from 20 years of age to current weight and HMW adiponectin levels (data not shown), suggesting a possibility that HMW adiponectin levels among the elderly are modulated by systemic energy valance [5–7]. Because weight decline (called *wasting*) is associated with an adverse cardiovascular outcome in elderly persons [8], high levels of HMW adiponectin might also reflect harmful signals in the body in advanced age [5,6].

4.2. Des-acyl ghrelin and atherosclerosis in elderly hypertensives

In contrast to HMW adiponectin, the inverse correlation between des-acyl ghrelin and obesity was particularly strong in our subjects with advanced aged (≥75 years). The mechanisms responsible for the reduction of des-acyl ghrelin in obesity remain unknown, but at least two possible explanations could be considered. First, the decreased activity of acylation enzyme or increased activity of endogenous esterase may occur in obesity. Barazzoni et al. reported that abdominal fat accumulation leads to accelerated ghrelin acylation in conjunction with a decrease in the des-acyl ghrelin levels [19]. Our study did not measure the plasma level of acylated ghrelin, because the measurement of this parameter is technically complex (e.g., acidified plasma with a 1/10 volume of 1N HCl is needed), and thus this hypothesis remains untested. Second, the decreased des-acyl ghrelin level may be a consequence of unmeasured abnormal adipochemokines or physiological adaptation to the positive energy balance associated with obesity. Further research is needed in this area.

In the current study, the des-acyl ghrelin level showed a negative correlation with cIMT independently of age, WC, sex, smoking, 24-h BP and renal function. Because the des-acyl ghrelin level parallels the acylated ghrelin level [15], our data may simply confirm those of the previous report in which decreased total ghrelin levels were associated with the progression of cIMT in elderly patients with metabolic syndrome [20]. However, numerous studies suggest that des-acyl ghrelin itself shows a wide array of cardiovascular activities [10–14], and thus des-acyl ghrelin may exert independent effects on the cardiovascular system. The pathologic pathways linking des-acyl ghrelin and cIMT remain unclear, and are probably not related to factors such as hemodynamic, metabolic or inflammatory pathways. That des-acyl ghrelin was significantly correlated only with the NO_x level suggests the possibility that des-acyl ghrelin may increase NO bioactivity. This consideration is supported by the recent report of Tesauro et al., which demonstrated that administration of des-acyl ghrelin reversed endothelial dysfunction by increasing NO bioactivity [13]. Des-acyl ghrelin is as effective as ghrelin in activating intracellular signaling pathways (i.e., ERK-

1/2, Akt) [14] that could be involved in endothelial NO production. However, our data indicate that the association of des-acyl ghrelin with atherosclerosis is independent from the NO_x level, thus the mechanisms responsible for this phenomenon could not be clarified in the present investigation. Nevertheless, because previous experiments showed a cardiovascular protective effect of des-acyl ghrelin [12–14], it is feasible that des-acyl ghrelin protects against the development of atherosclerosis. The atherosclerotic risks of abdominal obesity in our elderly persons were largely explained by elevated 24-h BP and reduced des-acyl ghrelin levels, suggesting the possibility that an increase in the des-acyl ghrelin level, in addition to BP control, may counteract the obesity-related atherosclerosis in elderly persons.

Our study has several limitations. First, because of the cross-sectional nature of our data, we cannot infer any causality. Hopefully longitudinal follow-up data will be able to provide some insights. Second, because our study was conducted in elderly hypertensives, caution should be used in applying the results to different groups. Third, all cardiometabolic parameters were measured only once. Finally, medication use may be potentially confounding, although our results were not changed after adjustment of these factors as a covariate.

In conclusion, the current study has demonstrated that the plasma des-acyl ghrelin level is a suitable predictor of cardiovascular risk in elderly hypertensives. The prognostic value of this peptide with respect to cardiovascular events will be addressed in a follow-up study in the present study population. In addition, the cardiovascular protective effect of des-acyl ghrelin suggests that the peptide could play a modulating role in atherosclerosis, especially in obese subjects. Further intervention studies will be needed to clarify this possibility.

Acknowledgments

This study was partly supported by a grant-in-aid from the Foundation for the Development of the Community (Y.Y.). The authors are grateful for the dedicated work of our staff. We also thank T. Nagatomo, K. Kai, E. Kusao, M. Kawano, T. Hidaka, G. Nakamura, and S. Matsuda for their excellent support.

Appendix A. Supplementary data

Supplementary data associated with this article can be found, in the online version, at doi:10.1016/j.atherosclerosis.2008.10.013.

References

[1] Heiat A, Vaccarino V, Krumholz HM. An evidence-based assessment of federal guidelines for overweight and obesity as they apply to elderly persons. Arch Intern Med 2001;161:1194–203.
[2] Trujillo ME, Scherer PE. Adipose tissue-derived factors: impact on health and disease. Endocrinol Rev 2006;27:762–78.
[3] Matsuzawa Y, Funahashi T, Kihara S, Shimomura I. Adiponectin and metabolic syndrome. Arterioscler Thromb Vasc Biol 2004;24:29–33.
[4] Pischon T, Girman CJ, Hotamisligil GS, Rifai N, Hu FB, Rimm EB. Plasma adiponectin levels and risk of myocardial infarction in men. JAMA 2004;291:1730–7.
[5] Wannamethee SG, Whincup PH, Lennon L, Sattar N. Circulating adiponectin levels and mortality in elderly men with and without cardiovascular disease and heart failure. Arch Intern Med 2007;167:1510–7.
[6] Kadowaki T, Yamauchi T, Kubota N. The physiological and pathophysiological role of adiponectin and adiponectin receptors in the peripheral tissues and CNS. FEBS Lett 2008;582:74–80.
[7] Kubota N, Yano W, Kubota T, et al. Adiponectin stimulates AMP-activated protein kinase in the hypothalamus and increases food intake. Cell Metab 2007;6:55–68.
[8] Wedick NM, Barrett-Connor E, Knoke JD, Wingard DL. The relationship between weight loss and all-cause mortality in older men and women with and without diabetes mellitus: the Rancho Bernardo study. J Am Geriatr Soc 2002;50:1810–5.
[9] Pajvani UB, Du X, Combs TP, et al. Structure-function studies of the adipocyte-secreted hormone Acrp30/adiponectin. Implications fpr metabolic regulation and bioactivity. J Biol Chem 2003;278:9073–85.
[10] Kojima M, Hosoda H, Date Y, Nakazato M, Matsuo H, Kangawa K. Ghrelin is a growth-hormone-releasing acylated peptide from stomach. Nature 1999;402:656–60.
[11] Nakazato M, Murakami N, Date Y, et al. A role for ghrelin in the central regulation of feeding. Nature 2001;409:194–8.
[12] Kleinz MJ, Maguire JJ, Skepper JN, Davenport AP. Functional and immunocytochemical evidence for a role of ghrelin and des-octanoyl ghrelin in the regulation of vascular tone in man. Cardiovasc Res 2006;69:227–35.
[13] Tesauro M, Schinzari F, Iantorno M, et al. Ghrelin improves endothelial function in patients with metabolic syndrome. Circulation 2005;112:2986–92.
[14] Baldanzi G, Filigheddu N, Cutrupi S, et al. Ghrelin and des-acyl ghrelin inhibit cell death in cardiomyocytes and endothelial cells through ERK1/2 and PI 3-kinase/AKT. J Cell Biol 2003;159:1029–37.
[15] Akamizu T, Shinomiya T, Irako T, et al. Separate measurement of plasma levels of acylated and desacyl ghrelin in healthy subjects using a new direct ELISA assay. J Clin Endocrinol Metab 2005;90:6–9.
[16] Otsuki M, Hashimoto K, Morimoto Y, Kishimoto T, Kasayama S. Circulating vascular cell adhesion molecule-1 (VCAM-1) in atherosclerotic NIDDM patients. Diabetes 1997;46:2096–101.
[17] The committee to evaluate diagnostic standards for metabolic syndrome 2005 Definition and the diagnostic standard for metabolic syndrome. Nippon Naika Gakkai Zasshi 2005;94:794–809 [in Japanese].
[18] Inelmen EM, Sergi G, Coin A, Miotto F, Peruzza S, Enzi G. Can obesity be a risk factor in elderly people? Obes Rev 2003;4:147–55.
[19] Barazzoni R, Zanetti M, Ferreira C, et al. Relationships between desacylated and acylated ghrelin and insulin sensitivity in the metabolic syndrome. J Clin Endocrinol Metab 2007;92:3935–40.
[20] Kotani K, Sakane N, Saiga K, et al. Serum ghrelin and carotid atherosclerosis in older Japanese people with metabolic syndrome. Arch Med Res 2006;37:903–6.

Circ J 2009; **73**: 892–898

Effects of Long-Term Intravenous Administration of Adrenomedullin (AM) Plus hANP Therapy in Acute Decompensated Heart Failure

— A Pilot Study —

Toshio Nishikimi; Tsuyoshi Karasawa*; Chikako Inaba; Kimihiko Ishimura; Kazuyoshi Tadokoro; Shogo Koshikawa; Fumiki Yoshihara**; Noritoshi Nagaya†; Hideaki Sakio*; Kenji Kangawa†; Hiroaki Matsuoka

Background: It was reported previously that 30 min administration of adrenomedullin (AM) improves hemodynamics in chronic stable heart failure patients. The present study was designed to examine whether long-term AM+human atrial natriuretic peptide (hANP) administration can be used as a therapeutic drug in patients with acute decompensated heart failure (ADHF) in clinical setting.

Methods and Results: Seven acute heart failure patients (74±5 years) with dyspnea and pulmonary congestion were studied. AM ($0.02\mu g \cdot kg^{-1} \cdot min^{-1}$)+hANP ($0.05\mu g \cdot kg^{-1} \cdot min^{-1}$) was infused for 12 h and then hANP ($0.05\mu g \cdot kg^{-1} \cdot min^{-1}$) was infused for 12 h. Hemodynamic, renal, hormonal and oxidative stress responses were evaluated. AM+hANP significantly reduced mean arterial pressure, pulmonary arterial pressure and systemic and pulmonary vascular resistance without changing heart rate, and increased cardiac output for most time-points compared with those at baseline. In addition, AM+hANP reduced aldosterone, brain natriuretic peptide and free-radical metabolites compared with those at baseline (all $P<0.05$). AM+hANP increased urine volume and $U_{Na}V$ compared with baseline data.

Conclusions: In this small, pilot trial, AM+hANP therapy had beneficial hemodynamic and hormonal effects in ADHF. Intravenous infusion of AM with hANP could be used as a therapeutic drug in ADHF. These data are preliminary and require confirmation in a larger clinical study. (*Circ J* 2009; **73**: 892–898)

Key Words: Acute decompensated heart failure; Adrenomedullin; Atrial natriuretic peptide; Brain natriuretic peptide; Oxidative stress

Adrenomedullin (AM), a strong vasodilatory peptide, was originally isolated from human pheochromocytoma[1] Infusion of AM causes vasodilatation, diuresis and natriuresis in normal animals[2] AM also increases cardiac output and left ventricular contractility in vivo and exerts a direct inotropic effect in vitro[3] We and others have shown that plasma AM levels are increased in patients with congestive heart failure[4,5] Tissue levels of the AM peptide and mRNA have also been shown to be increased in the heart, kidney and lungs of rats with congestive heart failure[6] These findings suggest that AM may play a role in the regulation of volume and pressure homeostasis in congestive heart failure as a paracrine and/or autocrine factor, and as a circulating hormone. In addition, we reported previously beneficial hemodynamic and renal effects of AM infusion in animals with congestive heart failure[7] In humans, systemically administered AM has been shown to decrease mean arterial pressure (MAP) significantly in healthy subjects without any adverse effects[8] These findings raise the possibility that intravenous infusion of AM may also be beneficial in human subjects with heart failure. Indeed, we and other investigators demonstrated previously that short-term infusion of AM increased the cardiac index (CI) and decreased mean pulmonary arterial pressure (mPA) only in patients with chronic stable heart failure[9,10] In comparison with human atrial natriuretic peptide (hANP), AM is more potent in decreasing vascular resistance and enhancing cardiac output, and less potent in diuresis and natriuresis[11] The infusion of hANP is currently used as a treatment for acute decompensated heart failure (ADHF) in Japan; however, some of the patients with ADHF are resistant to hANP monotherapy. Taken together, these results suggest that AM+ANP therapy may be used as a therapeutic drug in ADHF. However, it is not known whether long-term AM+ANP infusion in ADHF is beneficial or not.

Therefore, our aim in the present study was thus to investigate if long-term AM+ANP infusion therapy was effective in terms of hemodynamics, renal function and hormone levels in patients with ADHF in a real clinical setting.

(Received May 19, 2008; revised manuscript received December 11, 2008; accepted December 17, 2008; released online April 2, 2009)
*Department of Hypertension and Cardiorenal Medicine, *Department of Intensive and Critical Care Medicine, Dokkyo Medical University, Mibu, **Department of Medicine, National Cardiovascular Center and †Research Institute National Cardiovascular Center, Suita, Japan*
Mailing address: Toshio Nishikimi, MD, Department of Hypertension and Cardiorenal Medicine, Dokkyo University School of Medicine, Mibu 321-0293, Japan. E-mail: nishikim@dokkyomed.ac.jp
All rights are reserved to the Japanese Circulation Society. For permissions, please e-mail: cj@j-circ.or.jp

Methods

The present study was approved by the ethics committee of the Dokkyo Medical University, and all patients gave written informed consent.

Study Subjects

Seven patients with ADHF who were admitted to our hospital with a prime complaint of dyspnea were studied. Chest X-rays in all patients showed cardiomegaly with pulmonary congestion. After written informed consent was obtained, baseline blood tests and echocardiography were performed. Patients with one of the following conditions were excluded: (1) chronic renal impairment (serum creatinine level 2.0 mg/dl); (2) systolic blood pressure <100 mmHg; or (3) the presence of aortic stenosis or mitral stenosis. The baseline clinical characteristics and hemodynamics in the present study are shown in **Table**.

Preparation of Human AM

Human AM was obtained from Peptide Institute Inc, Osaka, Japan. The homogeneity of human AM was confirmed using reverse-phase, high-performance liquid chromatography and amino acid analysis. AM was dissolved in saline with 4% D-mannitol and sterilized through a 0.22-μm filter (Millipore Co, Billerica, MA, USA). Then, randomly selected vials were submitted for sterility and pyrogen testing, as reported previously.[10] The chemical nature and content of the human AM in the vials were verified using high-performance liquid chromatography and radioimmunoassay.

Study Protocol

All patients were hospitalized in our intensive care unit. A 7.5-F Swan-Ganz catheter (TOO21H-7.5F, Baxter Co, Deerfild, IL, USA) was positioned in the pulmonary artery through a jugular vein. One 22-gauge cannula was inserted into a radial artery for hemodynamic measurements and blood sampling. Another 22-gauge cannula was inserted into a forearm vein for the infusion of 0.9% hANP, with or without AM. A bladder catheter was inserted for urine sampling. During an equilibration period of 60 min, baseline hemodynamic, renal and blood samples for hormonal measurements were obtained. Then, AM ($0.02\mu g \cdot kg^{-1} \cdot min^{-1}$)+hANP ($0.05\mu g \cdot kg^{-1} \cdot min^{-1}$) were administered intravenously at a rate of 0.5 ml/min for 12 h, followed by 12 h of hANP ($0.05\mu g \cdot kg^{-1} \cdot min^{-1}$) infusion (**Figure 1**). Hemodynamic parameters, including heart rate (HR), MAP, mPA, pulmonary capillary wedge pressure (PCWP) and cardiac output, were continuously monitored and measured at 60-min intervals during the protocol. Blood samples were taken before, 12 h after AM+hANP infusion and 12 h after hANP monotherapy. Urine samples were obtained every 60 min. Urine volume, urinary sodium excretion, urinary potassium excretion, urinary cAMP and cGMP excretion were measured and calculated using standard formulas.

Table. Patient Characteristics

Age (years)	74±5
M/F	5/2
BMI (kg/m^2)	25.7±5.2
NYHA (III/IV)	5/2
Cause of HF (IHD/valvular)	4/3
BNP (pg/ml)	1,350±1,187
Cre (mg/dl)	1.0±0.5
Echocardiographic findings	
LVDd	61±6
LVDs	46±8
EF	39±10
MR (II/III/IV)	2/1/4
AR (III)	1
Baseline hemodynamic data	
MAP	98±17
SVR	1,699±529
CI	2.54±0.80
HR	73±14
mPA	45±15
PAR	370±252
PCWP	27±9

BMI, body mass injdex; NYHA, New York Heart Association; HF, heart failure; MAP, mean arterial pressure; SVR, systemic vascular resistance; CI, cardiac index; HR, heart rate; mPA, mean pulmonary arterial pressure; PAR, pulmonary arterial resistance; PCWP, pulmonary capillary wedge pressure.

Hormone and Oxidative Stress Marker Measurement

Plasma total AM, mature AM, atrial natriuretic peptide (ANP) and brain natriuretic peptide (BNP) levels were measured using immunoradiometric assays with a specific kit for each marker (Shionogi Co, Ltd, Osaka, Japan).[11] Plasma cyclic adenosine 3', 5'-monophosphate (cAMP), cyclic guanosine 3', 5'-monophosphate (cGMP), renin, aldosterone and norepinephrine (NE) were measured with commercially available kits.[12] Reactive oxygen metabolite (d-ROM) was

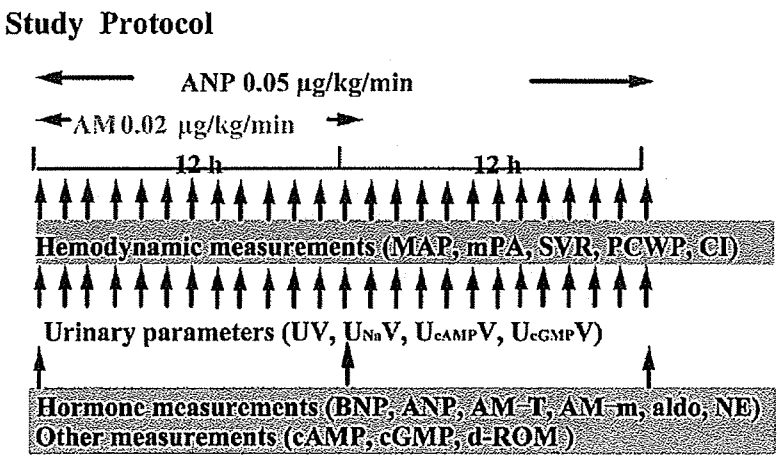

Figure 1. Study protocol. After a 60-min baseline period, AM ($0.02\mu g \cdot kg^{-1} \cdot min^{-1}$)+hANP ($0.05\mu g \cdot kg^{-1} \cdot min^{-1}$) was administered intravenously for 12 h, followed by hANP ($0.05\mu g \cdot kg^{-1} \cdot min^{-1}$) monotherapy for 12 h. AM, adrenomedullin; AM-m, AM-mature; AM-T, AM-total; ANP, atrial natriuretic peptide; BNP, brain natriuretic peptide; cAMP, cyclic adenosine 3', 5'-monophosphate; CI, cardiac index; cGMP, cyclic guanosine 3', 5'-monophosphate; d-ROM, reactive oxygen metabolite; hANP, human atrial natriuretic peptide; MAP, mean arterial pressure; mPA, mean pulmonary arterial pressure; NE, norepinephrine; PCWP, pulmonary capillary wedge pressure; SVR, systemic vascular resistance.

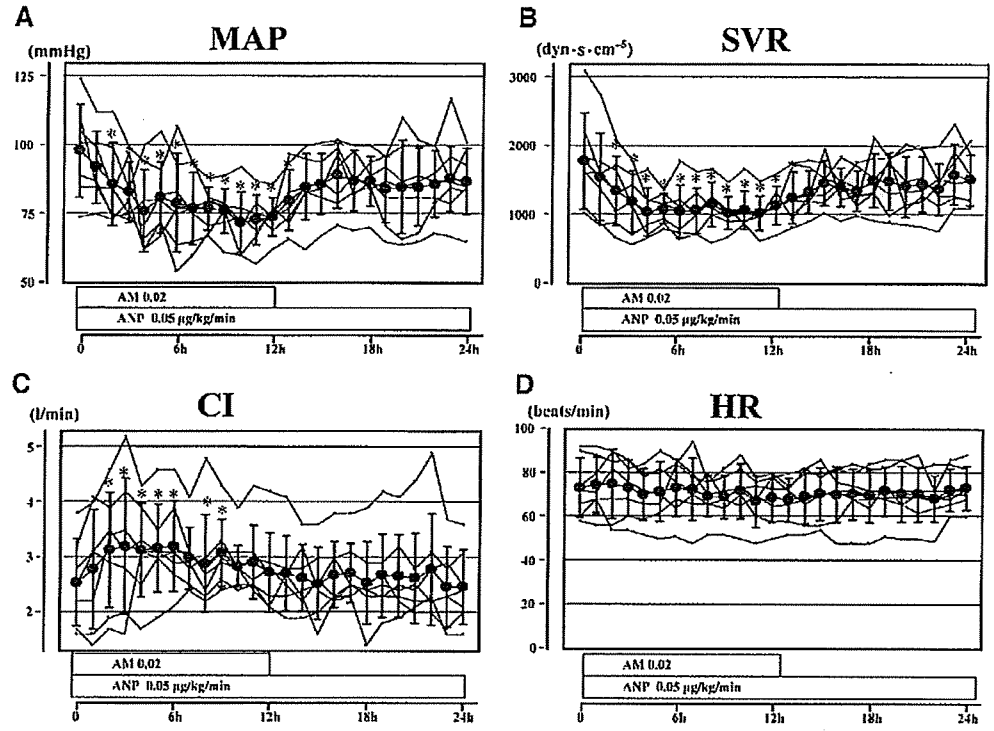

Figure 2. Systemic hemodynamic [(A) MAP, (B) SVR, (C) CI and (D) HR] changes during the infusion of AM+hANP and hANP therapy. Data are mean±SD. *P<0.05 vs value at time 0. HR, heart rate. Other abbreviations see in Figure 1.

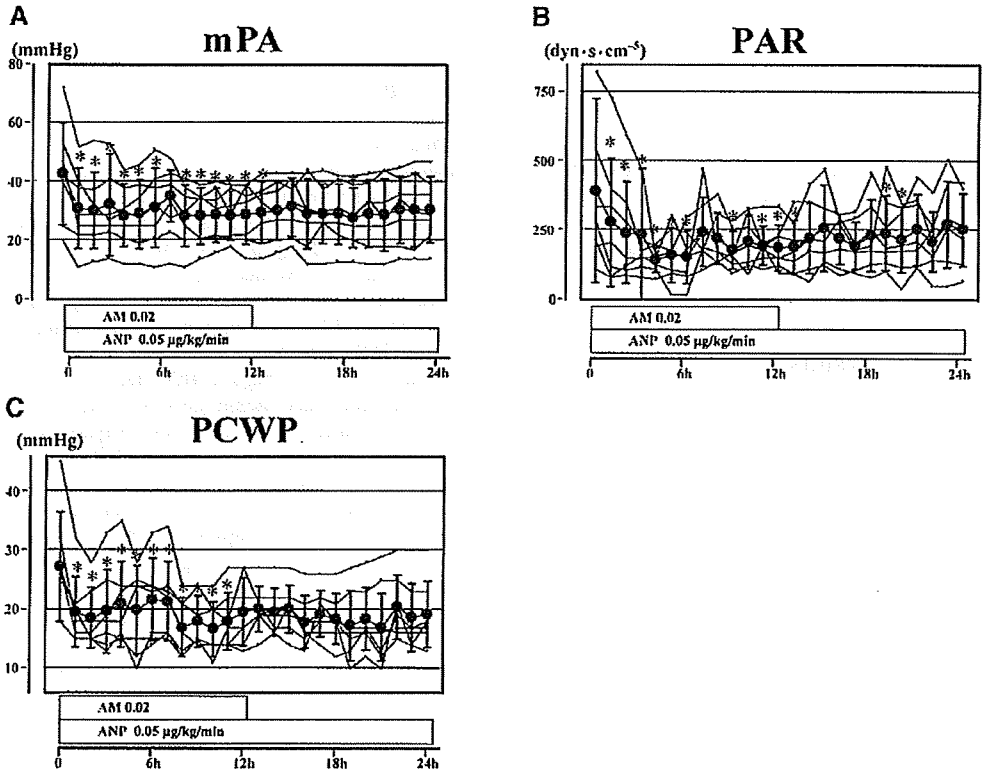

Figure 3. Pulmonary hemodynamic [(A) mPA, (B) PAR and (C) PCWP] changes during the infusion of AM+hANP and hANP therapy. Data are mean±SD. *P<0.05 vs value at time 0. PAR, pulmonary arterial resistance. Other abbreviations see in Figure 1.

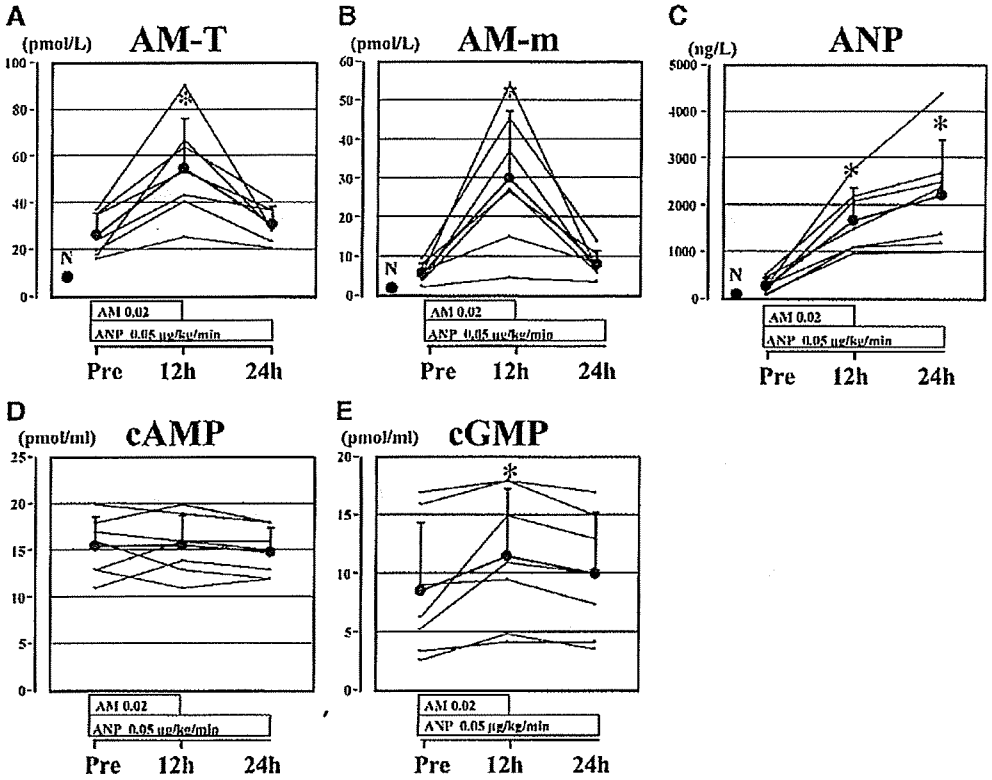

Figure 4. Hormonal [(A) AM-T, (B) AM-m, (C) ANP, (D) cAMP and (E) cGMP] changes during infusion of AM+hANP and hANP therapy. Data are mean±SD. *P<0.05 vs value at time 0. Abbreviations see in Figure 1.

measured using a commercially available kit (H&D, s.r.l., Parma, Italy).

Statistical Analysis

All data were expressed as mean±SD unless otherwise indicated. Comparisons of the parameters between the baseline data and each time point were made using a paired Student's t-test. Log transformation was completed for plasma BNP and ANP levels. P<0.05 was considered statistically significant.

Results

All subjects tolerated the present study protocol. No obvious side effects were observed in blood chemistry tests such as liver function, renal function, electrolytes or hemograms. The 2 of 7 patients had mild skin flushing in the body during the AM+hANP therapy. This disappeared soon after switching to ANP monotherapy.

Hemodynamic Responses to AM and hANP

The infusion of AM+hANP significantly decreased MAP, systemic vascular resistance (SVR), and increased CI (**Figures 2A–C**) at most of the time-point compared with the baseline levels, whereas there were no changes in HR (**Figure 2D**). Infusion of AM+hANP also significantly decreased mPA, pulmonary vascular resistance and PCWP at most time-points compared with the baseline values (**Figures 3A–C**).

Hormonal and Oxidative Stress Responses to AM and hANP

Baseline plasma total AM, mature AM and ANP were significantly elevated in patients with heart failure and were comparable with previous reports (**Figures 4A–C**). At the end of AM+hANP infusion, plasma total AM, mature AM and ANP increased about 2-fold, 6-fold and 6-fold, respectively. After switching to hANP monotherapy, plasma total AM and mature AM decreased to near baseline levels, whereas plasma ANP increased further (**Figures 4A–C**).

Infusion of AM+hANP significantly increased the plasma level of cGMP, which is a secondary messenger for ANP, BNP and nitric oxide (**Figure 4E**). Plasma levels of cAMP, one of the secondary messengers of AM, did not change significantly during the study period (**Figure 4D**).

The effects of infusion of AM+hANP on plasma BNP, aldosterone, NE, PRA, and d-ROM are shown in **Figure 5**. Infusion of AM+hANP significantly decreased plasma BNP and aldosterone levels (**Figures 5A,B**). In contrast, NE or PRA levels did not change (**Figures 5C,D**). Interestingly, the infusion of AM+hANP significantly decreased d-ROM levels, a marker of oxidative stress (**Figure 5E**).

Renal Urinary Responses to AM and hANP

Infusion of AM+hANP tended to increase urine volume, urinary sodium excretion and urinary cAMP excretion compared with the baseline level and these changes reached statistical significance at several points; however, there seemed to be no differences in these parameters between AM+hANP and hANP monotherapy. Whereas urinary cGMP excretion was significantly higher for almost entire period compared

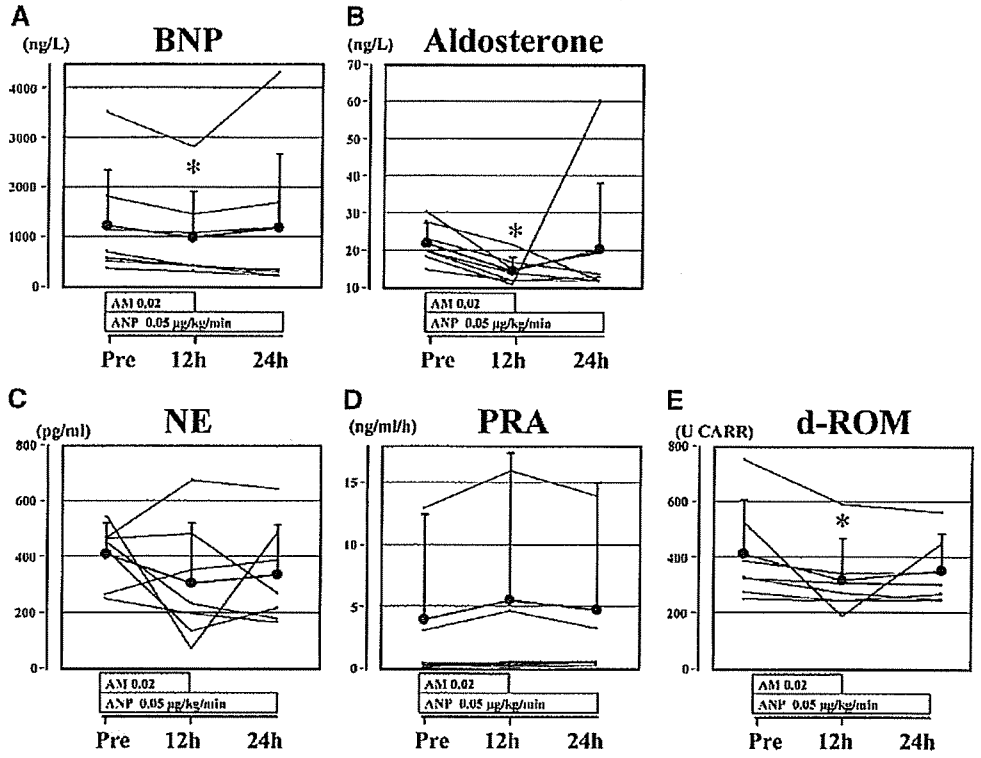

Figure 5. Hormonal [(A) BNP, (B) aldosterone, (C) NE and (D) PRA] and (E) oxidative stress marker (d-ROM) changes during the infusion of AM+hANP and hANP therapy. Data are mean±SD. *P<0.05 vs value at time 0. Abbreviations see in Figure 1.

with the baseline level (data not shown).

Discussion

In our small pilot trial, the administration of combined AM+hANP in patients with ADHF was effective in reducing MAP, SVR, mPA, PAR, PCWP, BNP, aldosterone and d-ROM, and in increasing CI, UV, $U_{Na}V$, $U_{cAMP}V$ and $U_{cGMP}V$. These results suggest that long-term AM+hANP infusion may be an effective treatment for patients with ADHF in a real clinical setting due to the reduction of systemic and pulmonary vascular resistance, positive inotropic effects, inhibitory action of aldosterone secretion and oxidative stress production.

In the present study, AM+hANP therapy significantly decreased SVR, MAP, PAR and mPA without changing HR. Previous studies have demonstrated that AM directly dilated vascular smooth muscle cells in a cAMP-dependent manner![13] A further study also showed that AM dilates vessels via a cGMP cascade with the production of nitric oxide![14,15] In the present study, plasma cAMP levels did not increase, maybe due to the low dose of AM ($0.02\mu g \cdot kg^{-1} \cdot min^{-1}$), because our previous studies showed that higher doses of AM ($0.05\mu g \cdot kg^{-1} \cdot min^{-1}$) increased plasma cAMP levels in patients with chronic heart failure and pulmonary hypertension![10,16] Thus, whether plasma cAMP increased or not appeared to depend on the dose of AM used. HR did not increase in the present study. Previous studies have demonstrated that AM induced an increase of HR![10] This discrepancy of the results between two studies may be explained by the two reasons: (1) a low dose of AM ($0.02\mu g \cdot kg^{-1} \cdot min^{-1}$) was used in the present study compared with the previous study ($0.05\mu g \cdot kg^{-1} \cdot min^{-1}$); and (2) hANP was concominantly used in the present study. Because hANP is known to exert a sympathoinhibitory action in heart failure, AM-induced reflex-mediated sympathetic activation may be blunted. Thus, a combination of AM+hANP would aid HR stability through mutual effects![17]

In the present study, AM+hANP therapy increased CI. Because AM+hANP therapy reduced SVR and PAR significantly, the observed increase of CI may be in part due to a reduction of afterload. In addition, several reports demonstrated that AM has positive inotropic effects. Szokodi et al reported that AM enhances cardiac contractility via cAMP-independent mechanisms, including a Ca^{2+} release from intracellular ryanodine- and thapsigargin-sensitive Ca^{2+} stores, activation of protein kinase C and Ca^{2+} influx through L-type Ca^{2+} channels![18] In agreement with these findings, Nagaya et al demonstrated that intravenous AM enhances left ventricular myocardial contraction and improves left ventricular relaxation without increasing myocardial oxygen consumption in patients with left ventricular dysfunction![19] Thus, positive inotropic effects from AM, not mediated via the cAMP/PKA pathway, may be useful in the treatment for ADHF.

Interestingly, AM+hANP therapy reduced BNP, aldosterone and d-ROM levels. The reduction of BNP is considered to be due to hemodynamic improvement, including reduction of SVR, PAR and PCWP![20] Interestingly, AM+hANP therapy reduced plasma aldosterone levels. Previous studies demonstrated that AM inhibits aldosterone production induced by angiotensin II, potassium and Ca^{2+} ion-